Synthesis, characterization, and electrogenerated chemiluminescence of phenyl-substituted, phenyl-annulated, and spirofluorenyl-bridged oligothiophenes

Ullrich Mitschke and Peter Bäuerle *

Department of Organic Chemistry II (Organic Materials and Combinatorial Chemistry), University of Ulm, Albert-Einstein-Allee 11, D-89081 Ulm, Germany. E-mail: peter.baeuerle@chemie.uni-ulm.de; Fax: +49-731-502-2840

To overcome the insolubility of higher oligothiophenes and simultaneously to enhance their processability with respect to an application in molecularly doped organic light-emitting devices (OLEDs) we synthesized phenyl-substituted, phenyl-annulated, and spirofluorenyl-bridged oligothiophenes **1**–**5**. Significantly improved solubilities in polar solvents of up to three orders of magnitude were found and their optical and electrochemical properties were investigated in solution. Reflecting small conformational changes and the almost complete electronic separation of the substituents, phenyl substitution and the introduction of a spiro core by bridging the central bithienyl unit only slightly affected optical and redox properties in comparison to the unmodified oligothiophenes (**6**–**8**). In contrast, the presence of an isothianaphthene (benzo[*c*]thiophene) unit in the oligomeric chain led to a distinct approximation of the frontier orbitals and consequently to a red-shift of both absorption and fluorescence. Finally, we demonstrated the applicability of some oligomers as dopants for OLEDs by electrogenerated chemiluminescence (ECL).

Introduction

On the basis of their chemical stability and ease of functionalization, thiophene-based oligomers are a subject of intense research activities.[1] Although oligothiophenes were initially studied as model compounds to gain insight into the structural and electronic peculiarities of the corresponding polydisperse polymers, thin films thereof have also served as active media in highly efficient organic field-effect transistors (FETs)[2] and organic light-emitting devices (OLEDs).[3] Typically, the ease of sublimative processing has been taken advantage of, and the oligomeric material has been introduced by vacuum evaporation into the electronic device. The performance of early thiophene-based OLEDs was affected by the intrinsic *p*-type character of the electron-rich oligothiophenes, making them suitable for hole transport but not applicable for electron transport.[3a] This behaviour inevitably led to ill-balanced charge carrier injection in electroluminescence devices. In recent publications we demonstrated a strengthening of the electron affinity of thiophene-based oligomers by introducing electronegative heteroatoms such as oxygen and nitrogen into the conjugated chain.[4] Preliminary attempts to produce electrooptical devices substantiated the usefulness of this approach and allowed improvements of the external quantum efficiency of thiophene-based OLEDs by more than one order of magnitude upon insertion of an electron transport layer of a thiophene–1,3,4-oxadiazole oligomer.[3a] Besides the possibility of building up multilayer configurations with separated hole and electron transport layers in successive sublimative steps, the incorporation of different compounds into polymeric matrices (*e.g.* polystyrene) represents another reasonable approach to overcoming the ill-balanced charge carrier injection in simple oligothiophene-based OLEDs.[3a,5] This approach derives benefit from an easy separation of the essential functions of fluorescence, hole and electron transport and their assignment to different organic materials. The introduction of low molecular weight materials as molecular dopants into polymeric matrices

presupposes processability from solution and typically requires preparation techniques like spin- or dip-coating which demand a good solubility of the materials applied. Typically, the solubility of thiophene-based oligomers has been increased by the introduction of alkyl substituents at both α- and β-positions of the thiophene rings, which however is often accompanied by structural consequences in the solid state.[1a] In thin film FETs, for instance, alkyl side groups proved to have a significant impact on film morphology.[2] Macroscopic properties such as conductivity and charge carrier mobility critically depend on the ordering effect of the alkyl groups on the one hand and their isolating nature on the other hand.[2,6] Moreover, the introduction of alkyl or alkoxy side chains in conjugated polymers proved to enhance the device performance of OLEDs by virtue of chain separation and hence impedance of the formation of non-emissive relaxation sites.[3a] However, in amorphous composite OLEDs with a low degree of molecular order and a small density of chromophores the isolating nature of alkyl side groups—detrimental to charge transport—prevails and may disadvantageously affect device performance. Herein, we report on different approaches to improve the solubility and hence processability of higher oligothiophenes to make them applicable as hole transport emitters for polymer-based composite OLEDs. Attaching aromatic moieties in different positions and in distinct types of connection to the conjugated system we test phenyl substitution (**1** and **2**), phenyl annulation (**3**) and the incorporation of a central spiro core (**4** and **5**) as promising structural modifications in order to induce a higher solubility of oligothiophenes.

With respect to an application as molecular dopants for composite OLEDs particular attention is paid to the optical and electrochemical properties of oligomers **1**–**5** in comparison to their unmodified analogues, "end-capped" oligothiophenes EC*n*T (EC4T **6**, EC5T **7**, EC6T **8**)[7] which show a dramatic loss of solubility with increasing conjugation length.

Phenyl-substituted oligothiophenes have rarely been reported in the literature. Among them, differently phenyl-substituted

DOI: 10.1039/b006553f

1 R = Ph, R′ = H
2 R, R′ = Ph

3 R——R′ =

4 n = 0
5 n = 1

EC*n*T 6-8 (n = 2-4)
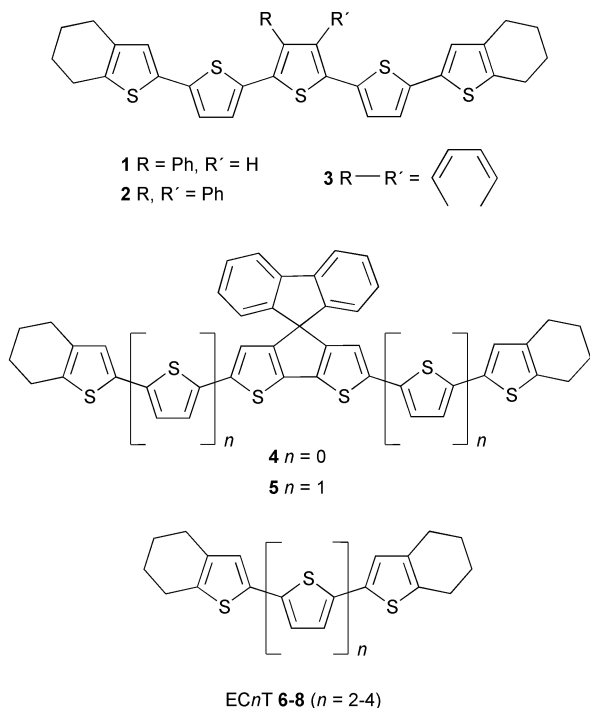
terthiophenes were investigated with respect to their steric constraints and strongly twisted non-planar structures were found.[8] Several patents of Fuji Electric Co. deal with materials for xerographic applications having phenyl-substituted oligothienyl segments.[9] A lot of work has been done concerning phenyl-substituted polythiophenes, especially poly(3-phenylthiophene) and its derivatives.[3a,10,11] Their regioselective synthesis,[10a,b] the influence of different substitution patterns at the phenyl units on the electrochemical properties,[10c] and their conductivities in both the neutral and the doped state are well reported. In some cases good solubility[10d] and stabilization effects were observed rendered possible by extended conjugation.[10e,f] Poly(3-phenylthiophene)s were used in non-linear optical studies[11a] and as active materials in OLEDs.[3a] Furthermore, they were suggested as potential materials for electrochemical capacitors[11b,c] and charge storage applications.[11d] The solubilizing effect of phenyl substituents was also used in another class of conjugated polymers to provide higher processability. Phenyl-substituted poly(*p*-phenylenevinylene)s can be incorporated into electronic devices by simple coating techniques.[3a]

Substituted benzo[*c*]thiophene oligomers up to the tetramer[12] and trimeric combinations of thiophene and (functionalized) benzo[*c*]thiophene units[13] were synthesized as model compounds and monomers for corresponding low band gap polymers. Recently, Cava *et al.* synthesized a wide range of even longer mixed oligomers composed of thiophene and benzo[*c*]thiophene units and investigated their optical and electrochemical properties.[14] In comparison to the oligothiophene analogues enhanced solubility and significant red-shifts of absorption and emission were found.

Providing a rigid 90° geometry, spiro-units have lately been used to perpendicularly connect electronically separated conjugated oligomers. Tour *et al.* synthesized orthogonally fused conjugated systems for molecular scale electronic devices using a spirobithiophene moiety with a central silicon atom or a 9,9′-spirobifluorene as core segments and attached oligothienylene or oligothienyleneethinylene chains as branches to four connecting sites.[15] The spiro-concept has quite recently been used to ensure the morphological stability of organic electroluminescent materials. Salbeck *et al.* synthesized spiro-linked compounds suitable as emitter, hole transport, or electron transport materials for organic electroluminescent devices[16] and suggested some of them as materials for molecular solid-state lasers.[16a] Recently, Schmidt *et al.* presented an amorphous hole

blocking material with a high glass transition temperature based on triazine units affixed to a central spirobiindan core.[17] Both groups succeeded in fabricating highly efficient OLEDs using spiro-linked compounds as active materials.[16b,c,17]
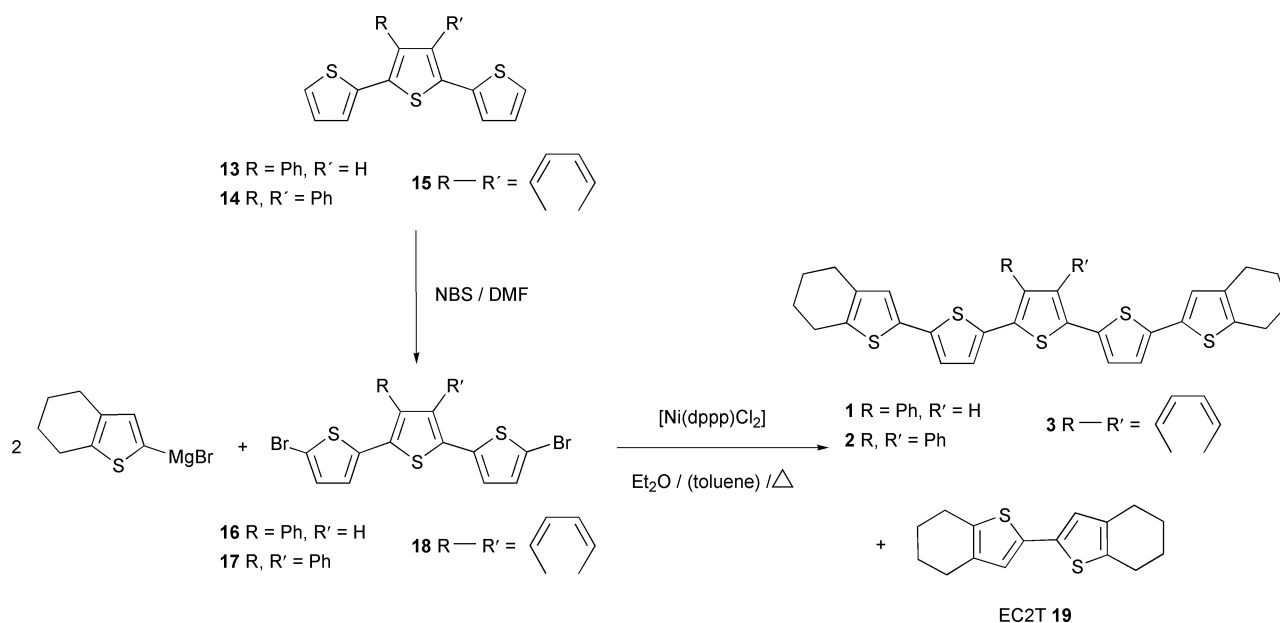
Results and discussion

Synthesis

All target structures **1**–**5** were synthesized *via* final transition metal-catalyzed cross-coupling reactions. The synthesis of appropriately functionalized building blocks started from 3-phenylthiophene (**9**)[18] and 3,4-diphenylthiophene (**10**),[19] respectively, in which bromo substituents were introduced at the 2- and 5-positions by reaction with two equivalents of *N*-bromosuccinimide (NBS) in DMF (80 and 90% yield, Scheme 1).

9 R = Ph, R′ = H
10 R, R′ = Ph

11 R = Ph, R′ = H
12 R, R′ = Ph

13 R = Ph, R′ = H
14 R, R′ = Ph
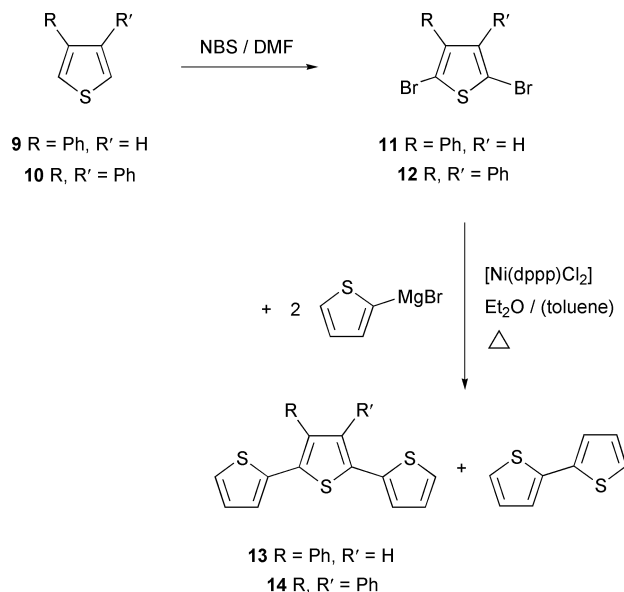
Scheme 1 Synthesis of phenyl-substituted terthiophenes **13** and **14**.

The subsequent Kumada-type nickel-catalyzed cross-coupling reaction of **11** and **12** with two equivalents of 2-thienylmagnesium bromide in diethyl ether led to the corresponding terthiophenes **13** and **14**, respectively (Scheme 1). Surprisingly, the formation of the aryl–aryl bonds was more difficult than expected. Due to their steric demands the phenyl substituents evidently disturb the ideal geometry of the catalytic active species. In the case of disubstituted trimer **14** up to six equivalents of Grignard component were necessary to achieve a complete reaction. However, this also promoted the formation of 2,2′-bithiophene as homocoupling product which was quantitatively removed by distillation. Chromatographic work-up of the raw material gave the required terthiophenes **13** and **14** in yields of 53 and 47%. By reaction with two equivalents of NBS in DMF the introduction of bromine atoms at the terminal α-positions of the latter terthiophenes afforded dibromoterthiophenes **16** and **17** nearly quantitatively, in 94 and 99% yield, respectively (Scheme 2).

Subsequently, two equivalents of the Grignard reagent of 2-bromo-4,5,6,7-tetrahydrobenzo[*b*]thiophene were coupled with dibromoterthiophenes **16** and **17** under nickel catalysis. Although the phenyl substituents in **16** and **17** are not in immediate proximity to the catalytic centre, again up to six equivalents of Grignard compound were necessary to accomplish the reaction. The necessity of using arylmagnesium halides in significant excess in order to build up longer oligomers has previously been reported for quinquethiophene,[20] alkyl-substituted quinque-,[21] and sexithiophenes[22] and their typical low solubility is an obvious handicap. In spite of the
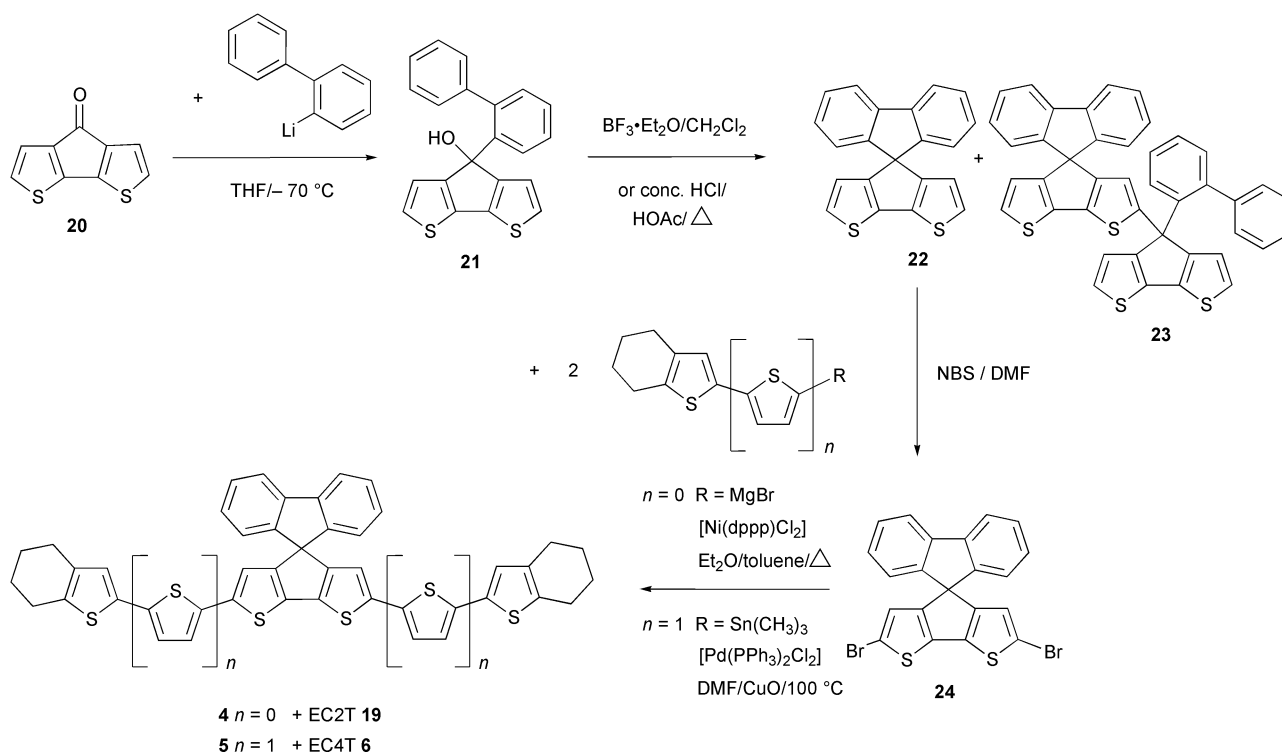
13 R = Ph, R′ = H
14 R, R′ = Ph
15 R — R′ =

NBS / DMF

16 R = Ph, R′ = H
17 R, R′ = Ph
18 R — R′ =

[Ni(dppp)Cl₂]

Et₂O / (toluene) /△

1 R = Ph, R′ = H
2 R, R′ = Ph
3 R — R′ =

EC2T **19**

Scheme 2 Synthesis of phenyl-substituted and benzo[*c*]annulated oligothiophenes **1**–**3**.

larger amount of homocoupling product EC2T **19** generated by reacting the Grignard component in excess, phenyl-substituted quinquethiophenes **1** and **2** could be easily purified and separated from **19** by chromatography. Fractionated sublimation finally yielded 45 and 48% of analytically pure compounds **1** and **2**, respectively.

Following the same synthetic concept, by reaction with two equivalents NBS in DMF, bromo substituents were introduced at the α-positions of annulated terheterocycle **15**[13a] (Scheme 2). Taking into account that the isothianaphthene positions also possess reactivity towards electrophilic attack, the reaction was performed at −20 °C. Nevertheless, traces of isomers were formed, which could be removed quantitatively by recrystallization, affording neat dibromoterthiophene **18** in 69% yield. The synthesis of thiophene–isothianaphthene oligomer **3** was accomplished by means of a nickel-catalyzed cross-coupling of two equivalents of Grignard reagent of 2-bromo-4,5,6,7-

tetrahydrobenzo[*b*]thiophene with dibromoterthiophene **18**. Due to the excess of Grignard reagent (5 eq.), the main side product was again homocoupling product EC2T **19**. Due to its low solubility in diethyl ether–toluene, the major part of oligomer **3** precipitated from solution and was purified by chromatography in 43% yield. In sharp contrast to all other target compounds presented within this and previous publications,[4] sublimation of **3** failed and led to complete decomposition of the material which indicates a decrease of thermal stability by introduction of an isothianaphthene unit into the oligomeric chain.

The central building block for the synthesis of spirofluorenyl-bridged oligothiophenes **4** and **5** is spiro-compound **24**, available in a three-step synthesis starting from 4*H*-cyclopenta[2,1-*b*:3,4-*b*′]dithiophen-4-one (**20**)[23c] and 2-bromobiphenyl (Scheme 3). Transformation of the latter led to 2-lithiobiphenyl which could be reacted with ketone **20** at

20

THF/− 70 °C

21

BF₃·Et₂O/CH₂Cl₂

or conc. HCl/
HOAc/△

22

23

NBS / DMF

+ 2

n = 0 R = MgBr
[Ni(dppp)Cl₂]
Et₂O/toluene/△

n = 1 R = Sn(CH₃)₃
[Pd(PPh₃)₂Cl₂]
DMF/CuO/100 °C

24

4 *n* = 0 + EC2T **19**
5 *n* = 1 + EC4T **6**

Scheme 3 Synthesis of spirofluorenyl-bridged oligothiophenes **4** and **5**.

−70 °C to afford tertiary alcohol **21** in 83% yield. In the next step the spiro-core was formed by an intramolecular condensation reaction induced by either boron trifluoride–diethyl ether in dichloromethane or concentrated hydrochloric acid in acetic acid. Both reagents generate a triarylmethyl cation from alcohol **21**. Intramolecular electrophilic attack at the *ortho*-position of the terminal phenyl unit is favoured due to five-ring formation leading to spiro-compound **22**. Due to three stabilizing aryl units, the lifetime of the carbenium ion is long enough for the ion to also intermolecularly react at the α-thienyl position. Thus, independent of which dehydrating reagent was used, "dimer" **23** was identified as the main side product. The relative ratio of **22** to **23** and their absolute yield strongly depend on the dilution of the reaction mixture. Using boron trifluoride–diethyl ether at a concentration of 5×10^{-3} mol L^{-1} of alcohol **21**, 60% of spiro-compound **22** and 5% of "dimer" **23** were obtained after chromatographic work-up. Probably on account of the higher reaction temperature, the yield of **22** was diminished to 47% when concentrated hydrochloric acid in acetic acid was used as the condensation medium. Finally, the reaction of **22** with two equivalents of NBS in DMF afforded central coupling component **24** in 92% yield.

The synthesis of spirofluorenyl-bridged oligothiophene **4** was achieved by nickel-catalyzed cross-coupling reaction of **24** with two equivalents of the Grignard reagent of 2-bromo-4,5,6,7-tetrahydrobenzo[*b*]thiophene (Scheme 3). In order to improve the solubility of **24**, toluene was added to the reaction mixture. Again a large excess of the Grignard component was necessary to drive the reaction to completion. Homocoupling product EC2T **19** was separated by chromatography and subsequent sublimation finally gave **4** in 24% yield as analytically pure material. However, as indicated by the moderate yield, the limit of the Kumada-type nickel-catalyzed cross-coupling seemed to be almost reached with this size of component. Accordingly, analogous reaction of **24** with two equivalents of the corresponding bithienyl Grignard component afforded spirofluorenyl-bridged sexithiophene **5** in only 4% yield. However by applying a variant of the Stille reaction,[24] two equivalents of 5-(4,5,6,7-tetrahydrobenzo[*b*]thiophen-2-yl)-2-trimethylstannylthiophene were reacted with dibromide **24** and bis(triphenylphosphine)palladium(II) dichloride and copper(II) oxide as the catalytic system in DMF at 100 °C (Scheme 3). The reaction is strongly promoted by the cocatalyst CuO, guaranteeing completion within less than twenty hours. Since the excess of the organometallic component is significantly lower in comparison to the Kumada-type coupling reactions, homocoupling product EC4T **6** was formed in a distinctly smaller amount. Chromatography and subsequent sublimation gave pure spirofluorenyl-bridged end-capped sexithiophene **5** in 70% yield.

Solubilities of oligothiophenes 1–5

As a result of their low solubility, thiophene-based oligomers often lack sufficient processability. Nevertheless, oligothiophenes can be introduced as active components into electronic devices by sublimative deposition.[2,3] However, some applications demand coating or blending techniques and, hence, require good solubility of the oligomer as a prerequisite. Usually this problem has been overcome by *alkyl* substitution.[1] For instance, the solubility of a β-didecyl-substituted sexithiophene in chloroform is approximately 400 g L^{-1} and, therefore, at least four orders of magnitude higher than that of unsubstituted sexithiophene (< 0.05 g L^{-1}).[25] In order to quantify the solubilizing effect of *aromatic* substituents affixed to an oligothiophene backbone, we determined the saturation concentrations c_{sat} and solubilities of oligothiophenes **1–8** in dichloromethane at ambient temperature (Table 1).

Since solubilities include distinct molecular masses, the discussion is focused on the comparison of saturation concen-

Table 1 Saturation concentrations c_{sat} and solubilities of phenyl-substituted, benzo[*c*]annulated and spirofluorenyl-bridged oligothiophenes **1–5** in comparison to end-capped oligothiophenes EC*n*T **6–8** in dichloromethane at ambient temperature

	c_{sat}/mol L^{-1}	Solubility/g L^{-1}
1	1.4×10^{-2}	8.4
2	7.2×10^{-3}	4.9
3	1.7×10^{-2}	9.4
EC5T **7**	4.0×10^{-4}	0.21
4	2.0×10^{-2}	12
EC4T **6**	1.0×10^{-2}	4.6
5	4.9×10^{-3}	3.8
EC6T **8**	1.9×10^{-6}	1.1×10^{-3}

trations. The data obtained cover a wide range from extremely soluble for spiro-quaterthiophene **4** ($c_{sat} = 2.0 \times 10^{-2}$ mol L^{-1}) to nearly insoluble for EC6T **8** ($c_{sat} = 1.9 \times 10^{-6}$ mol L^{-1}). This reflects a rapidly decreasing solubility with increasing chain length of the oligothiophene scaffold. On account of their steric demands, the phenyl substituents in quinquethiophenes **1** and **2** are twisted with respect to the conjugated backbone. In comparison to unsubstituted quinquethiophene EC5T **7** intermolecular π–π interactions in the solid phase are therefore hampered. Consequently, the saturation concentrations of the phenyl-substituted oligothiophenes **1** and **2** exceed the value obtained for their unsubstituted analogue **7** by more than one order of magnitude. Due to the asymmetric molecular structure this effect is even more pronounced in the case of monophenyl derivative **1**. Although an explanation is less obvious, the incorporation of an isothianaphthene unit in **3** also leads to a significant improvement of the solubility compared with EC5T **7**. Annulation of a benzene ring probably induces a stronger polarization of the π-electron system and, hence, enables a better stabilization in polar solvents. The dramatic loss of solubility with increasing chain length is evident on comparing the data obtained for end-capped oligothiophenes **6–8**. Since end-capped quaterthiophene EC4T **6** ($c_{sat} = 10^{-2}$ mol L^{-1}) is still well dissolved in dichloromethane, the improvement of the solubility achieved by bridging the central bithiophene unit with a spirofluorenyl core in **4** is, as expected, minor. However, the solubilizing power of a central spiro-core becomes far more effective when the sexithiophene systems are compared. In spite of its distinctly higher molecular mass, spiro-compound **5** ($c_{sat} = 4.9 \times 10^{-3}$ mol L^{-1}) is more than three orders of magnitude more soluble than end-capped sexithiophene EC6T **8** ($c_{sat} = 1.9 \times 10^{-3}$ mol L^{-1}).

In summary, it can be concluded that all approaches, the incorporation of spiro-segments, the replacement of β-protons with phenyl substituents, and the annulation of a benzene ring, were successful with respect to a distinctly improved solubility in comparison to unsubstituted analogues. Although we did not find significantly altered trends in other solvents, these results are strictly valid for dichloromethane as solvent.

Optical characterization

The optical properties of phenyl-substituted, benzo[*c*]-annulated, and spirofluorenyl-bridged oligothiophenes **1–5** were studied in comparison to those of the parent oligomers EC*n*T **6–8**. The absorption and emission maxima, maximum extinction coefficients, fluorescence quantum yields, and the optical energy gaps are given in Table 2. Deconvolution of the absorption and emission bands allowed the determination of the 0–0 transitions and the Stokes shifts. The optical energy gaps correspond to the energy difference of the ground and the excited states and therefore correlate to the energetic gap of the frontier orbitals.

Broad and unstructured π–π* absorption bands were observed for pentamers **1–3**, reflecting the non-coplanarity and

Table 2 Optical properties of phenyl-substituted benzo[*c*]annulated, and spirofluorenyl-bridged oligothiophenes **1–5** in comparison to end-capped oligothiophenes EC*n*T **6–8**

	$\lambda_{max}^{abs\,a}$/nm	log (ε/l mol^{-1} cm^{-1})	$\lambda_{max}^{em\,a}$/nm	$\Phi_{295\,K}^{em\,b}$/%	$\Delta E_{opt.}^{c}$/eV	$\Delta\tilde{v}^{d}$/cm^{-1}
1	422	4.61	512, 536	19 (± 5)	2.54	1403
2	424	4.62	512, 536	21 (± 5)	2.53	1282
3	500	4.42	624, 668[e]	6 (± 2)	2.09	1400
EC5T **7**	431	4.71	499, 533	40 (± 5)	2.56	997
4	431	4.66	486, 516	27 (± 5)	2.62	870
EC4T **6**	408	4.61	471, 499	20 (± 5)	2.70	893
5	472	4.83	540, 579	37 (± 5)	2.36	967
EC6T **8**	444	4.79	521, 551	43 (± 5)	2.46	1049

[a] Solvent dichloromethane, $c = 5 \times 10^{-6}$ mol L^{-1} for absorption measurements, $c = 1 \times 10^{-6}$ mol L^{-1} for emission measurements. [b] External standard was fluorescein. [c] The energy gap was determined from the average of the 0–0 transitions in absorption and emission. [d] Stokes shift determined by deconvolution of the spectra. [e] Shoulder.
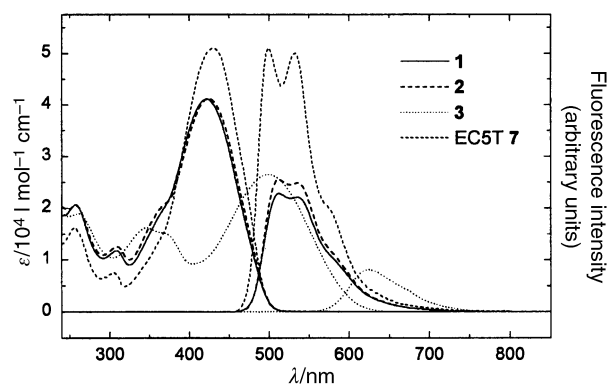
Fig. 1 Absorption and corrected emission spectra of phenyl-substituted and benzo[*c*]annulated oligothiophenes **1–3** in dichloromethane in comparison to end-capped quinquethiophene EC5T **7**, $c = 5 \times 10^{-6}$ mol L^{-1} (abs.) and 1×10^{-6} mol L^{-1} (em.).

rotational freedom of the individual rings in the aromatic system (Fig. 1). With respect to quinquethiophene EC5T **7**, absorption is only slightly blue-shifted by phenyl substitution ($\Delta\lambda_{7,1}^{abs} = -9$ nm, $\Delta\lambda_{7,2}^{abs} = -7$ nm) but significantly red-shifted by introduction of a benzo[*c*]thiophene segment ($\Delta\lambda_{7,3}^{abs} = +69$ nm). The latter observation is in accordance with previously reported results concerning the shifts of absorption maxima that have been observed upon replacement of the central thiophene moiety by a benzo[*c*]thiophene unit in terthiophene ($\Delta\lambda^{abs} = +77$ nm)[13a] and quinquethiophene ($\Delta\lambda^{abs} = +66$ nm), respectively.[14] Due to the electron-donating effect of the cyclohexene caps in thiophene–benzo[*c*]thiophene oligomer **3**, the absorption maximum ($\lambda_{max}^{abs} = 500$ nm) is slightly displaced to lower energies in comparison to the analogous non-capped system ($\lambda_{max}^{abs} = 482$ nm (dichloromethane)).[14]

Phenyl substitution causes a decrease of the extinction coefficient for the π–π* band. Nevertheless, compared to EC5T **7** the oscillator strength in the spectrum of **1** and **2** is approximately maintained since transitions at $\lambda = 257$, 308, and ≈ 360 nm clearly gain intensity. Interestingly, as the similar absorption spectra of **1** and **2** indicate, this change does not take place stepwise but is already realized for monophenyl substitution. Regarding the absorption spectrum of thiophene–isothianaphthene oligomer **3**, the decrease of the extinction coefficient is even more pronounced, leading to a broad and similarly intense absorption that covers, with exception of the red region, the whole visible range.

In accordance with the absorption, the spectral range of the fluorescence is only marginally affected by the presence of phenyl substituents. Nevertheless, in comparison to EC5T **7** the emission maxima of phenyl- and diphenyl-substituted pentamers **1** and **2** are slightly shifted to lower energies ($\Delta\lambda_{7,1}^{em} = \Delta\lambda_{7,2}^{em} = +13$ nm). Since absorption is hypsochromically and emission bathochromically displaced, phenyl substituents destabilize the electronic ground state but have a stabilizing

effect on the first excited state. In accordance with this observation the Stokes shifts of **1** and **2**, determined by deconvolution of the absorption and emission spectra, are somewhat higher than the value obtained for EC5T **7**, indicating a greater geometric change in the excited state. With respect to the fluorescence intensity of quinquethiophenes **1**, **2**, and **7**, phenyl substitution has an even more pronounced effect since the fluorescence quantum yield is significantly diminished upon introduction of phenyl substituents. In accordance with the absorption, the emission maximum of thiophene–benzo[*c*]-thiophene oligomer **3** is slightly red-shifted with respect to its non-capped analogue ($\Delta\lambda^{em} = +11$ nm)[14] and distinctly bathochromically displaced in comparison to end-capped quinquethiophene EC5T **7** ($\Delta\lambda_{7,3}^{em} = +125$ nm). With respect to the related highly fluorescent trimer 1,3-di(2-thienyl)benzo[*c*]-thiophene ($\Phi^{em}_{295\,K} = 57(\pm 2)$%),[13a] the extension of the conjugated system by two additional thiophene units in **3** ($\Phi^{em}_{295\,K} = 6(\pm 2)$%) significantly diminishes the fluorescence intensity. Evidently, small structural changes can dramatically alter the relative distribution to different relaxation paths. This is in sharp contrast to the continuous increase of the fluorescence quantum yield with increasing chain length that has been reported for both the end-capped[7] and non-substituted[26] oligothiophene series. The optical energy gaps, which correspond to the energy of the 0–0 transition, are nearly identical for phenyl-substituted pentamers **1** and **2**, reflecting the similarity of their absorption and emission spectra. Since the determined optical energy gap of EC5T **7** deviates only slightly from these values, phenyl substitution only marginally influences the energetic separation of the frontier orbitals. However, the annulation of a benzene ring in **3** strongly affects the electronic structure and leads to a significant decrease of the energy gap ($\Delta E^{opt.}_{7,3} = -0.47$ eV).

The planarization of the central bithienyl units in **4** and **5**, induced by the spirofluorenyl bridge, enhances the effective conjugation and in comparison to EC4T **6** and EC6T **8** causes a significant red-shift of both absorption ($\Delta\lambda_{6,4}^{abs} = +23$ nm, $\Delta\lambda_{8,5}^{abs} = +28$ nm) and emission ($\Delta\lambda_{6,4}^{em} = +15$ nm, $\Delta\lambda_{8,5}^{em} = +19$ nm). Due to the stiffer molecular structure, single vibronic couplings and shoulders of the absorption and emission bands are more pronounced than in the case of oligomers **1–3** (Fig. 2).

Both compounds **4** and **5** show an intense second absorption band at $\lambda_{max}^{abs} = 266$ nm, which corresponds to the absorption of the fluorene moiety. Moreover, in accordance with its unbridged analogue EC6T **8**, spiro-hexamer **5** reveals another absorption band at $\lambda_{max}^{abs} = 329$ nm. While the intensity of the fluorene absorption is maintained, the addition of two additional thiophene units to the oligomeric backbone enhances the intensity of the longest wavelength π–π* absorption, as expected. On account of the presence of two orthogonally separated π-systems, the fluorescence of tetramer **4** and hexamer **5** is not independent with respect to the excitation wavelength. The spectra shown in Fig. 2 correspond to an excitation in the range of the π–π* absorption of the oligo-

Table 3 Electrochemical properties of phenyl-substituted, benzo[*c*]annulated, and spirofluorenyl-bridged oligothiophenes **1–5** in comparison to end-capped oligothiophenes EC*n*T **6–8**

	$E^{\circ}_{Red2}{}^{a}$/V	$E^{\circ}_{Red1}{}^{a}$/V	$E^{\circ}_{Ox1}{}^{b}$/V	$E^{\circ}_{Ox2}{}^{b}$/V	$E^{\circ}_{Ox3}{}^{b}$/V	$\Delta E_{EC}{}^{a,c}$/V	$\Delta E_{EC}{}^{b,c}$/V
1	−2.58[d]	−2.38	0.33	0.50	—	2.64	2.57
2	−2.63[d]	−2.44	0.31	0.48	—	2.65	2.58
3	−2.32	−2.01	0.11	0.38	—	2.03	1.97
EC5T **7**	−2.58[d]	−2.33	0.25	0.51	—	2.56	2.44
4	≈−2.78[e]	−2.58	0.18	0.57	—	2.67	2.59
EC4T **6**	−2.75[e]	−2.49	0.34	0.65	—	2.74	2.69
5	−2.43	−2.32	0.16	0.37	1.09[d]	2.40	2.32
EC6T **8**	−2.48	−2.31	0.22	0.41	—	2.46	2.38

[a] In THF–*n*Bu$_4$NPF$_6$ (0.1 M) *vs.* Fc/Fc$^+$ at 100 mV s^{-1}. [b] In dichloromethane–*n*Bu$_4$NPF$_6$ (0.1 M) *vs.* Fc/Fc$^+$ at 100 mV s^{-1}. [c] Determined by $\Delta E_{CV} = E'_{Ox1} - E'_{Red1}$ (E' is the potential at which the redox process starts) and solvent correction. [d] Quasireversible redox process. [e] Irreversible redox process, E° determined at $I' = 0.855 \times I_p$.[28]
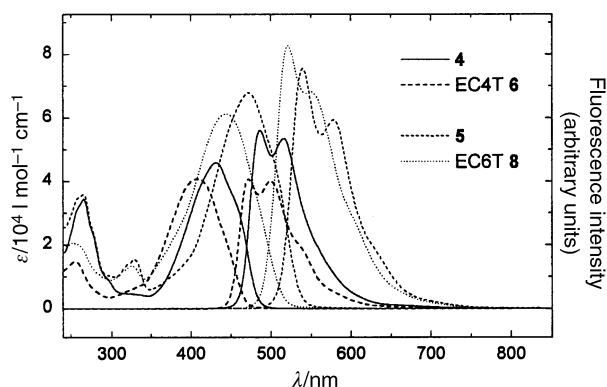
Fig. 2 Absorption and corrected emission spectra of spirofluorenyl-bridged oligothiophenes **4** and **5** in dichloromethane in comparison to end-capped oligothiophenes EC4T **6** and EC6T **8**, $c = 5 \times 10^{-6}$ mol L^{-1} (abs.) and 1×10^{-6} mol L^{-1} (em.).

thiophene unit. If the systems are excited within the range of the fluorene absorption band, the corresponding fluorescence spectra comprise two components. Interestingly, not only the fluorescence of the fluorene unit can be observed but also the fluorescence of the oligothiophene moiety. Since emission spectra were measured at a concentration of 1×10^{-6} mol L^{-1}, intermolecular energy transfer can be excluded as a possible explanation for this observation. Although the aromatic moieties are separated by an isolating quaternary carbon atom, intramolecular energy transfer across the spiro-core seems to be a possible relaxation path. The absolute fluorescence intensity is obviously hardly affected by the presence of the spirofluorene bridge. The fluorescence quantum yields of **4** and **5** only slightly deviate from the data obtained for end-capped oligothiophenes EC4T **6** and EC6T **8**, respectively.

Deconvolution of both absorption and emission spectra allowed the determination of the 0–0 transitions and, therefore, the evaluation of the energetic separation of the frontier orbitals. Reflecting the central planarized bithienyl unit, which guarantees a higher effective conjugation of the oligothiophene backbone, the energy gaps of oligomers **4** and **5** are decreased in comparison to their unbridged analogues EC4T **6** and EC6T **8**. The Stokes shifts, however, are only slightly affected by incorporation of the spiro-cores and remain in the range of $\Delta \tilde{\nu} \approx 800$–1000 cm^{-1}, indicating a relatively small geometric change in electronic excitation. In summary, it can be concluded that the optical properties of oligothiophenes are changed to different extents by distinct types of aromatic substituents in β-thienyl positions. Phenyl substitution only marginally affects absorption and emission but seems to have a stabilizing effect in the excited state. Extension of conjugation by benzo[*c*]annulation significantly changes the electronic structure and causes a strong red-shift of both absorption and emission. Finally, the forced planarization of bithienyl units by
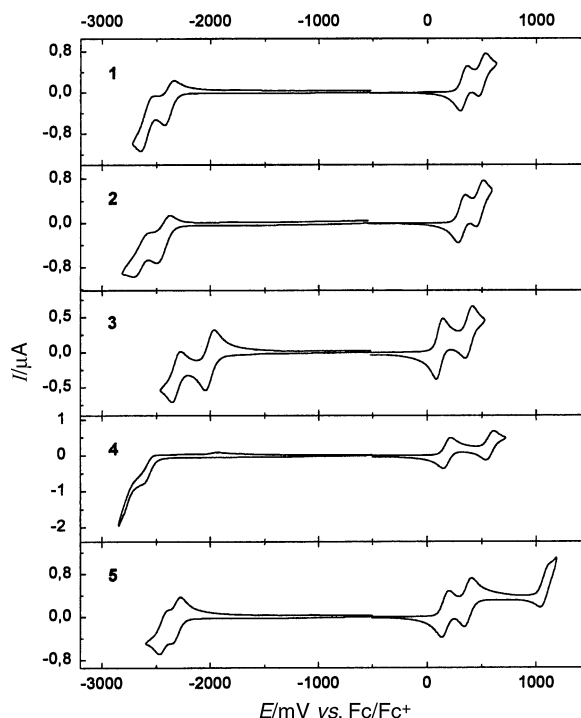
Fig. 3 Electrochemical characterization of phenyl-substituted, benzo[*c*]annulated, and spirofluorenyl-bridged oligoheterocycles **1–5**. Reduction in THF–*n*Bu$_4$NPF$_6$ (0.1 M), $c = 3.5 \times 10^{-4}$ mol L^{-1}; oxidation in dichloromethane–*n*Bu$_4$NPF$_6$ (0.1 M), $c = 2.5 \times 10^{-4}$ mol L^{-1}; $v = 100$ mV s^{-1}.

incorporation of spiro-linkages enhances the effective conjugation of the oligomeric chain and causes an approximation of the frontier orbitals.

Electrochemical characterization

Oxidation and reduction potentials provide information concerning the relative energetic positions of the frontier orbitals. Since the performance of electronic and electrooptical devices critically depends on an appropriate tuning of the electronic structure at interfaces,[2a,3a,27] they are of special importance for device design and device control. The electrochemical properties of oligomers **1–5** were studied in comparison to those of their unmodified analogues **6–8** by cyclic voltammetry. Oxidation and reduction potentials are summarized in Table 3 and corresponding cyclic voltammograms (CVs) are shown in Fig. 3.

CVs in the oxidative potential regime were recorded in the electrolyte dichloromethane–*n*Bu$_4$NPF$_6$ (0.1 M) and potentials are given *versus* the ferrocene/ferricenium (Fc/Fc$^+$) couple at scan rates of 100 mV s^{-1}. Reduction was performed in the electrolyte THF–*n*Bu$_4$NPF$_6$ (0.1 M).

In accordance with their unsubstituted analogue EC5T **7**, phenyl-substituted end-capped quinquethiophenes **1** and **2** reveal two reversible oxidation waves, one reversible reduction wave, and a second quasireversible reduction wave. However, on account of the steric demands of the substituents, effective conjugation of the oligomeric chain is decreased and both oxidation ($\Delta E^\circ_{Ox1/7,1} = +0.08$ V, $\Delta E^\circ_{Ox1/7,2} = +0.06$ V) and reduction ($\Delta E^\circ_{Red1/7,1} = -0.05$ V, $\Delta E^\circ_{Red1/7,2} = -0.11$ V) are rendered more difficult, indicating a lower degree of conjugation for phenyl-substituted pentamers **1** and **2** compared to EC5T **7**. Consequently, the electrochemically determined energy gaps, estimated from the onset of the first oxidation and reduction process, are somewhat shifted to higher energies. The introduction of a second phenyl substituent only marginally affects the position of the redox potentials and delivers, in accordance with the optical measurements, nearly identical data for quinquethiophenes **1** and **2**.

Comparing EC5T **7** and thiophene–isothianaphthene oligomer **3**, the extension of the conjugated systems by benzo[c]annulation also guarantees full reversibility of the second reduction to form a chemically stable dianion. Furthermore, both oxidation ($\Delta E^\circ_{Ox1/7,3} = -0.14$ V) and reduction ($\Delta E^\circ_{Red1/7,3} = +0.32$ V) are distinctly facilitated, resulting in a significantly lower energy gap ($\Delta\Delta E_{EC/7,3} = -0.53$ V in THF). The terminal cyclohexene caps in oligomer **3** enable reversibility and strongly diminish the oxidation potential due to their electron-donating inductive effect. In this respect, Cava *et al.* reported an irreversible oxidation at 0.89 V (*vs.* calomel) for the non-capped analogue.[14]

The electrochemical data obtained for spiro-compounds **4** and **5** reflect the higher effective conjugation due to the planarization of the central bithiophene unit, induced by the spirofluorenyl bridge. Consequently, the energy gaps are slightly decreased ($\Delta\Delta E_{EC/6,4} \approx -0.07$ V in THF, $\Delta\Delta E_{EC/8,5} = -0.06$ V in THF) in comparison with those of EC4T **6** and EC6T **8**. Analogously to EC4T **6**, the second reduction of tetramer **4** to the dianion is followed by a chemical reaction, as indicated by the irreversibility of the redox wave and the appearance of an additional signal at lower potentials, which can be associated with the reoxidation of a decomposition product. While reduction is slightly shifted to lower potentials ($\Delta E^\circ_{Red1/6,4} = -0.09$ V, $\Delta E^\circ_{Red1/8,5} = -0.01$ V), oxidation is distinctly facilitated for both spiro-compounds **4** and **5** in comparison with end-capped oligomers **6** and **8** ($\Delta E^\circ_{Ox1/6,4} = -0.16$ V, $\Delta E^\circ_{Ox1/8,5} = -0.06$ V). Comparing **4** and **5**, the addition of two thiophene units only marginally affects the position of the first oxidation but significantly reduces the reduction steps and enables the reversibility of the second reduction. Furthermore, hexamer **5** is the only compound to show a third (quasireversible) oxidation at 1.09 V *vs.* Fc/Fc⁺.

In summary, the electrochemical characterization confirmed and underlined results previously deduced from the optical investigations. Phenyl substitution only marginally affects the energetic position of the frontier orbitals. Benzo[c]annulation, however, strongly modifies the electronic structure and decreases the energy gap significantly. On account of planarization, the electron-donating character of oligothiophenes is strengthened by incorporation of a spiro-core leading to decreased oxidation and only slightly shifted reduction potentials. Finally, electrochemically determined energy gaps are in good agreement with the corresponding values obtained by optical characterization.

### Electrogenerated chemiluminescence (ECL)

The fundamental processes in organic light-emitting diodes, charge creation, migration, and recombination, are decisively determined by charged states in the active organic layer.[3a,27] With regard to a potential application in OLEDs, ECL experiments represent a versatile tool with which to obtain valuable information concerning radical ion stability and electroluminescence intensity of suitable compounds. An ECL cell is essentially a miniaturized three-electrode single-compartment cell filled with an electroluminescent composition placed in the sample area of a fluorescence spectrometer. The ECL composition contains the fluorophore, a supporting electrolyte (nBu$_4$NPF$_6$), and a solvent (THF) that needs to be electrochemically inert over a wide range of potential, to include both oxidation and reduction potentials of the electroluminescent species (in the case of THF this prerequisite is fulfilled for oligothiophenes **3**–**7**). In the ECL experiment radical cations and anions are generated in successive electrochemical pulses. Excited fluorescent states of the active organic material can relax under light emission and hence electroluminescence may be reached *via* an electron transfer between oppositely charged radical ions in solution. This emission can be simultaneously monitored and compared to the photoluminescence of the species investigated (Fig. 4, left). Moreover, time-resolved fluorescence studies reveal the durability of the ECL and the relative stability of the radical ions involved (Fig. 4, right). Depending on this relative stability, to a certain extent irreversible follow-up products may be formed during the experiments which from time to time cause some electrode fouling. Nevertheless, these experiments provide helpful information in order to estimate the suitability of oligoheterocycles **3**–**7** to serve as an active organic material in OLEDs.

The ECL of quinquethiophene EC5T **7** approximately coincides with its photoluminescence (Fig. 4, left). However, the hypsochromic part of the electroluminescence spectrum is presumably underestimated due to readsorption processes of the electrolyte which in comparison to the optical experiments arise from the at least 50-fold higher concentration of the oligomer in the ECL experiments. On account of the scan rate of the fluorimeter on the one hand and the pulse rate k_p at which the system is exposed to oxidative and reductive conditions on the other hand, the ECL spectra are strongly structured due to the applied experimental conditions. ECL spectra structured to a smaller extent are typically obtained with pulse frequencies beyond 2 Hz or, alternatively, with slower scan rates of the fluorimeter. However, particularly in the case of end-capped quinquethiophene **7** high pulse rates were found to favor a rapid decrease of the light output as a consequence of a strongly accelerated decomposition of the ECL system. Since the continuous degradation of the ECL composition—though to a smaller extent—can also be observed at low pulse rates, slower scan rates of the fluorescence spectrometer are problematic with respect to a larger amount of cycles involved. Hence, an overvaluation of the hypsochromic, earlier recorded part of the spectrum becomes evident.

In order to estimate the durability of the ECL system and the relative stability of the radical species involved, time-resolved ECL spectra were recorded for compounds **3**–**7** (Fig. 4, right). EC5T **7** loses the major part of its initial light intensity within a small number of cycles. Although high pulse rates lead to rapid degradation of the electroluminescent composition, at least at a pulse rate of two seconds, the degradation of an EC5T-based cell is comparatively slow and remains at 30 to 40% of the initial light output within the first 50 cycles.

With strong and weak signals in turn, ECL compositions of EC5T **7** exhibit a specific pattern of time-resolved fluorescence indicating different persistences of the radical cation and anion involved. In the absence of suitable reactants, the relative persistence of radical cations and anions can be interpreted in terms of their relative stability. In the case of EC5T **7** the pulse sequence oxidation–reduction was found to exhibit distinctly higher light intensity than the sequence reduction–oxidation. This observation can be explained by a higher stability of the radical cation. The longer the lifetime of a radical ion, the more intense is the light output as a consequence of annihilation of oppositely charged radicals when the potential is switched
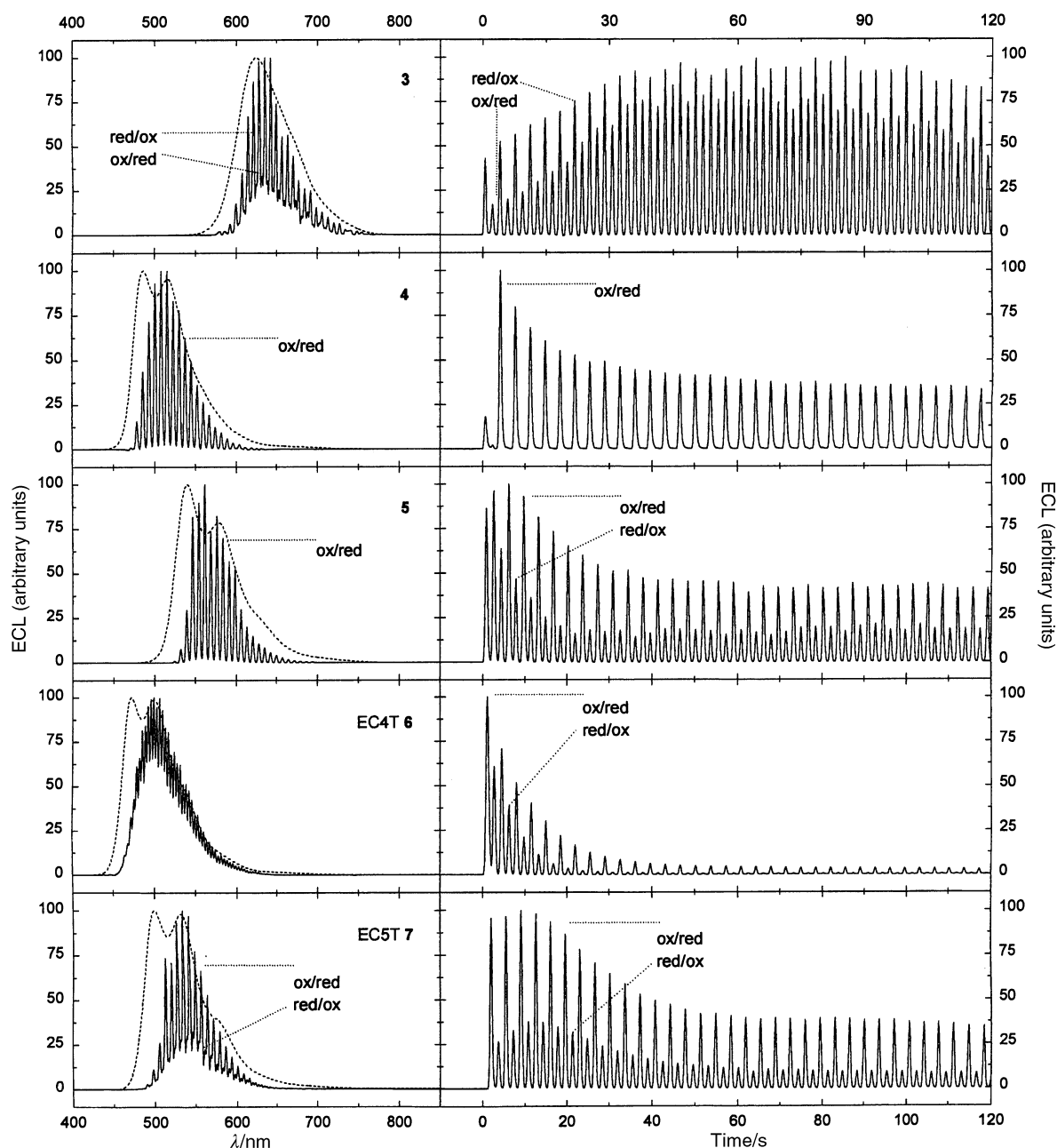
Fig. 4 Wavelength (left; **3**–**5**, EC5T **7**: $k_p = 2$ s; EC4T **6**: $k_p = 1$ s) and time-resolved (right; **3**: $\lambda_{Em} = 633$ nm, **4**: $\lambda_{Em} = 506$ nm, **5**: $\lambda_{Em} = 560$ nm, EC4T **6**: $\lambda_{Em} = 499$ nm, EC5T **7**: $\lambda_{Em} = 525$ nm; $k_p = 2$ s) ECL spectra of oligothiophenes **3**–**7** in THF–nBu$_4$NPF$_6$ (0.1 M), $c = 5 \times 10^{-4}$ mol L^{-1}; potentials applied: **3**: -1.70 V/$+0.74$ V, **4**: -2.30 V/$+0.80$ V, **5**: -1.97 V/$+0.82$ V, EC4T **6**: -2.20 V/$+0.95$ V, EC5T **7**: -2.08 V/$+0.94$ V *vs.* Ag/AgCl; scan rate = 120 nm min^{-1}; for comparison, the photoluminescence spectra (in dichloromethane) are depicted (dotted lines). Relative corrected fluorescence intensities of the ECL maxima were 1 (**4**) : 1 (**6**) : 3 (**3**) : 20 (**7**) : 150 (**5**). For comparison and clarity, all ECL spectra have been normalized to 100 arbitrary units.

to the opposite direction. The instability of the radical anion obviously induces the complete disappearance of the light output of the pulse sequence reduction–oxidation within a small number of cycles. The prevalence of radical cations is important with respect to the application of oligothiophene **7** as an active component in OLEDs since it seems to be better suited for hole transport. This result affirms the presumption that the moderate efficiency of simple thin film oligothiophene OLEDs based on EC5T **7** may be the consequence of an ill-balanced charge carrier distribution and the preponderance of holes.[3a]

Although its fluorescence quantum yield in solution is rather low ($\Phi_{295\ K}^{em} = 6\%$), the benzo[c]annulated oligoheterocycle **3** exhibits weak but remarkably stable electrochemiluminescence which is almost insensitive to different and particularly high pulse rates. This is presumably the consequence of the highly reversible redox chemistry and the high stability of both radical ions of **3** involved.

The high stability of ECL compositions based on oligomer **3** is in sharp contrast to the results obtained for quaterthiophenes **4** and EC4T **6**, respectively. Both compounds exhibit intense but unstable electrochemiluminescence, which coincides with their photoluminescence (Fig. 4, left). Similarly to EC5T **7**, reabsorption processes in the ECL solution seem to affect the hypsochromic part of the ECL spectrum. The instability of their radical anions, particularly in the case of EC4T **6**, leads to a rapid decay of the light output of the ECL cell (Fig. 4, right). In both cases the critical step is obviously the pulse sequence reduction–oxidation which delivers barely detectable luminance even after a small number of cycles. Although this is particularly true in the case of spirofluorenyl-bridged derivative **4**, its ECL seems to be discernibly more stable compared to that of EC4T **6** with respect to a smaller rate of decay and a significantly higher stability to high pulse rates.

The sensitivity of the active organic material to high pulse rates can be further reduced by extension of the conjugated system. Spirofluorenyl-bridged sexithiophene **5** reveals the most durable and, moreover, the most intense electrochemiluminescence among all the systems examined. Although the emitted light has not been quantified and the light output of an ECL cell based on **5** is diminished to a level of approximately 40% of the initial value after 50 cycles, the absolute light intensity is still remarkably high and unequivocally more intense than that of any other compound investigated. However, the persistence of the radical cation seems to be still greater than that of the radical anion since the sequence oxidation–reduction guarantees distinctly higher light intensities than the opposite sequence (Fig. 4, right). Moreover, despite the highly reversible redox chemistry of sexithiophene **5**, the contribution of the pulse sequence reduction–oxidation gradually vanishes and, finally, completely disappears under continuous operation (Fig. 4, left). With respect to a potential application in OLEDs, this observation underlines the higher persistence of the oligothiophene radical cations. Nevertheless, the extension of the conjugation length obviously increases the stability of the anionic species. Although oligothiophene **5** may not provide balanced charge injection, it is doubtless better suited to perform electron transport than related oligothiophenes with shorter effective conjugation length. On account of the inherent instability of its radical anion, however, tetramer **4** is expected to act as a hole transport emitter rather than on electron transporting material.

In conclusion, the intensity and durability of the electrochemiluminescence of several end-capped oligothiophenes in solution and the relative stability of the radical ions involved were examined by electrogenerated chemiluminescence. Despite these studies being performed in solution, valuable information with respect to a potential application of these materials in solid state organic light-emitting diodes (OLEDs) is provided, since the same phenomena such as charge creation and recombination are addressed. In a forthcoming paper we will report on the successful incorporation of spiro-oligothiophenes **4** and **5** in OLEDs.[29] Except for thiophene–isothianaphthene oligomer **3**, all compounds investigated revealed a higher stability of the radical cation. With the instability of the radical anion increasing, a more rapid decay of electrochemiluminescence within a small number of pulses was observed, indicating an ill-balanced capability of charge carrier transport in electrooptical devices. On account of its highly reversible redox chemistry, spiro-compound **5** revealed the most durable and most intense electrochemiluminescence among all the systems investigated in this study.

Conclusions

Several approaches to overcoming the lack of solubility and processability of higher oligothiophenes by introduction of aromatic substituents have been presented. In consideration of potential electronic and electrooptical applications the solubilizing effect of phenyl substitution, benzo[*c*]annulation and spiro-linkages was investigated. In comparison with unsubstituted analogues, the effect of structural modification was examined with respect to the optical and electrochemical properties.

The syntheses of phenyl-substituted, benzo[*c*]annulated, and spirofluorenyl-bridged oligothiophenes were accomplished by transition metal-catalyzed aryl–aryl coupling reactions. All compounds showed significant improvements in solubility of up to four orders of magnitude in comparison to their unmodified counterparts. The solubilizing power of spiro-[cyclopenta[2,1-*b*:3,4-*b'*]dithiophene-4,9'-fluorene] segments is particularly promising and intriguing with respect to the possibility of solubilizing even longer oligomers and in view of the construction of soluble macromolecules with a perpendic-

ular connection of different oligomeric chains. Distinct types of attachment of aromatic moieties to β-oligothiophene positions change the physical properties of the conjugated systems to markedly different extents. Phenyl substitution causes only slight and insignificant changes of optical and electrochemical data. The incorporation of spiro-units strengthens the effective conjugation by planarization of bithiophene units, as reflected in a bathochromic shift of absorption and emission as well as lower oxidation potentials. Benzo[*c*]annulation strongly affects the electronic structure and causes a significant decrease of the energetic separation of the frontier orbitals. Finally, we demonstrated the applicability of some oligomers as dopants for OLEDs by electrogenerated chemiluminescence (ECL). Preliminary attempts to fabricate OLEDs by embedding oligothiophenes **2**, **4**, and **5** as hole transport emitters into the polymeric matrices of composite OLEDs substantiated the usefulness of the presented approach, delivering devices that emitted green, blue, and yellow light with brightnesses of more than $10\,000$ cd m^{-2} under continuous operation. These results will be specified in a forthcoming publication.[29]

Experimental

General remarks

Solvents and reagents were purified and dried by the usual methods prior to use. Thin-layer chromatography (TLC) was carried out on Polygram SIL and Polygram Alox plastic plates from Macherey & Nagel. Developed plates were dried and examined under a UV lamp. Preparative column chromatography was performed on glass columns of different sizes packed with silica gel 60 (particle sizes 0.040–0.063 and 0.063–0.200 mm, Merck) or aluminium oxide 90 (activity II–III, particle size 0.063–0.200 mm, Merck). Petroleum ether refers to the fraction of bp 40–60 °C. Melting points were determined with a Büchi B-545 melting point apparatus and are corrected. FT-IR spectroscopy was performed on a Perkin-Elmer Spectrum 2000 instrument. ¹H NMR spectra were recorded on Bruker AMX 500 (500 MHz) and AC 200 (200 MHz) spectrometers (with deuterated solvent as lock-in and tetramethylsilane as internal reference; abbreviations: BPh = biphenyl-2-yl, BTh = benzo[*c*]thiophene, CPDTh = 4*H*-cyclopenta[2,1-*b*:3,4-*b'*]dithiophen(e/yl), Fl = fluorene, Ph = phenyl, Th = thiophene/thienyl, THBTh = 4,5,6,7-tetrahydrobenzo[*b*]thiophen-2-yl, and TTh = terthiophene). ¹³C NMR spectra were recorded on Bruker AMX 500 (126 MHz) and AC 200 (50 MHz) spectrometers. Mass spectra were recorded with a Varian MAT 711 instrument. Ions were generated by electron impact (EI) or field desorption (FD). Elemental analyses were performed on an Elementar vario EL instrument (limit of experimental error: ± 0.3%). Saturation concentrations and solubilities were determined by mixing a precise amount of substance (1–25 mg) with dichloromethane at ambient temperature until complete dissolution occurred. Without heating the sample, the dissolution was promoted by ultrasound and stirring. Additional solvent was added in time periods of ten minutes to allow thermodynamic equilibrium. UV–VIS spectra were recorded on a Perkin-Elmer Lambda 19 instrument in 1 cm cuvettes. Fluorescence spectra were recorded with a Perkin-Elmer LS 50 instrument in 1 cm cuvettes. Fluorescence quantum yields were determined with respect to 9,10-diphenylanthracene ($\Phi_R^{em} = 0.85$ in cyclohexane)[30] or fluorescein ($\Phi_R^{em} = 0.90$ in 0.1 M NaOH).[31] The cyclic voltammetry experiments were performed with a computer-controlled EG & G PAR 273 potentiostat in a three-electrode single-compartment cell (5 mL). The platinum working electrode consisted of a platinum wire sealed in a soft glass tube with a surface of $A = 0.785$ mm², which was polished down to 0.5 m with Buehler polishing paste prior to use in order to obtain reproducible surfaces. The counter electrode consisted of a platinum wire; the reference was a Ag/AgCl second-

ary electrode. All potentials were internally referenced to the ferrocene/ferricenium couple. Argon 4.8 was used to purge all solutions before use. Routinely, a constant concentration of $0.5–3.5 \times 10^{-4}$ mol L^{-1} of electroactive species was used. The electrolyte consisted of either dichloromethane (pa, SDS), which was heated at reflux and distilled in the presence of sulfuric acid under argon and subsequently filtered through aluminium oxide (ICN Alumina B, Activity grade Super I) or anhydrous THF (Aldrich), which was heated at reflux and distilled from potassium under argon. The solvents were directly transferred by means of syringes to the electrochemical cell. The supporting salt was 0.1 M nBu$_4$NPF$_6$ from Fluka which was twice recrystallized from ethanol–water and dried in a high vacuum.

Electrogenerated chemiluminescence (ECL)

ECL experiments were performed with a computer-controlled Jaissle PG 10 bipotentiostat in a laboratory-built three-electrode single-compartment cell (20 mL) consisting of a quartz vessel sealed with a Teflon block which carried a gold large-area counter electrode, a platinum working electrode (active area 5 × 5 mm), and a miniaturized Ag/AgCl secondary electrode as reference. The working electrode for the ECL experiments was prepared in the same way as those for cyclic voltammetry. Efficient argon supply was ensured by virtue of two additional openings in the Teflon closure. In this configuration the cell enabled both ECL experiments with consecutive electrochemical pulses and simultaneous fluorescence spectroscopy as well as conventional cyclic voltammetry in order to determine the precise position of the redox potentials of the electroluminescent compound. Routinely, a constant concentration of 5×10^{-4} mol L^{-1} of the electroactive species was used. Solvent (THF) and supporting electrolyte were prepared as described above. All solutions were purged with Argon 4.8, first investigated in a conventional electrochemical cell, and then transferred to the ECL cuvette. The exact positions of the oxidation and reduction potentials were checked before starting the ECL experiment. Pulse potentials were fixed to values of typically 20–50 mV beyond the precise redox potentials. After having the working electrode adjusted towards the detector of the fluorescence spectrometer, time-resolved ECL spectra were recorded at pulse rates of 2 s and a suitable fixed emission wavelength close to the photoluminescence maximum. Thereupon, a freshly prepared solution was utilized to record ECL spectra with pulse rates of typically 2, 1, and 0.5 s at a fluorimeter scan rate of 120 nm min^{-1}.

Starting materials prepared according to literature procedures

2,2-Bis(2-iodo-3-thienyl)-1,3-dioxolane [mp 123–124 °C, yield 38%],[23c] bis(triphenylphosphine)palladium(II) dichloride [mp 269–273 °C, yield 97%],[32] 4H-cyclopenta[2,1-b:3,4-b']-dithiophen-4-one (20) [mp 135 °C, yield 55%],[23c] 3,4-dibromothiophene [bp 48–50 °C/5 × 10^{-2} mbar, yield 65%],[33] 3,4-diphenylthiophene (10) [mp 113 °C, yield 75%],[19] 1,2-di-(2-thenoyl)benzene [mp 149–150 °C, yield 96%],[13a] 1,3-di(2-thienyl)benzo[c]thiophene (15) [mp 99 °C, yield 85%],[13a] di(3-thienyl)methanol [mp 68–69 °C, yield 75%],[23a] 2,2-di(3-thienyl)-1,3-dioxolane [mp 113–114 °C, yield 94%],[23b,c] 3-phenylthiophene (9) [mp 91 °C, yield 75%],[18] 3-(3-thenoyl)-thiophene [mp 78–80 °C, yield 80%].[23a]

2,5-Dibromo-3-phenylthiophene (11)

Under exclusion of light, a solution of NBS (4.67 g, 26.2 mmol) in DMF (abs., 20 mL) was added dropwise to a solution of 3-phenylthiophene (9) (2.00 g, 12.5 mmol) in DMF (abs., 20 mL) at 0 °C. The resulting mixture was kept for 1 h at 0 °C and was then allowed to warm to room temperature. After completion (15 h) the reaction mixture was poured into water and extracted with dichloromethane. The organic phase was washed

with saturated NaHCO$_3$ solution and water and was dried (MgSO$_4$). After evaporation of the solvent, the crude product was purified by recrystallization from ethanol to give 11 (3.20 g, 80%) as colourless microcrystals, mp 38–39 °C; FT-IR (KBr): v = 3057 w, 1491 m, 1446 w, 1210 w, 985 s, 843 m, 827 m, 757 s, 694 s, 549 m, 476 m cm^{-1}; ^{1}H NMR (200 MHz, CDCl$_3$): δ = 7.36–7.54 (m, 5 H, 2–6$_{Ph}$-H), 7.02 (s, 1 H, 4$_{Th}$-H); ^{13}C NMR (50 MHz, CDCl$_3$): δ = 141.1 (C-1$_{Ph}$), 134.0 (C-3$_{Th}$), 131.7 (C-4$_{Th}$), 128.50, 128.45, 128.04 (C-2–6$_{Ph}$), 111.2, 107.7 (C-2,5$_{Th}$); EI-MS, m/z (%): 320 (56), 318 (100) [M$^+$], 316 (48), 159 (11), 158 (70) [M$^+$ − 2 Br], 114 (16), 113 (9), 79 (15); C$_{10}$H$_6$Br$_2$S (318.0): calc. C 37.77, H 1.90, S 10.08; found C 38.06, H 2.08, S 9.95%.

2,5-Dibromo-3,4-diphenylthiophene (12)

Thiophene 12 was prepared as described for 11 from NBS (10.4 g, 58.4 mmol) in DMF (abs., 40 mL) and 3,4-diphenylthiophene (10) (6.70 g, 28.3 mmol) in DMF (abs., 40 mL/15 h). Recrystallization from ethanol yielded 12 (10.1 g, 90%) as colourless microcrystals, mp 149 °C; FT-IR (KBr): v = 3065 w, 3024 w, 1509 m, 1482 m, 1442 m, 1029 m, 997 s, 775 s, 764 s, 698 s, 608 s cm^{-1}; ^{1}H NMR (200 MHz, CDCl$_3$): δ = 7.20–7.35 (m, 6 H, 2,4,6$_{Ph}$-H), 7.02–7.12 (m, 4 H, 3,5$_{Ph}$-H); ^{13}C NMR (50 MHz, CDCl$_3$): δ = 142.2 (C-1$_{Ph}$), 134.4 (C-3,4$_{Th}$), 130.1, 127.92 (C-2,3,5,6$_{Ph}$), 127.65 (C-4$_{Ph}$), 109.5 (C-2,5$_{Th}$); EI-MS, m/z (%): 396 (54), 394 (100) [M$^+$], 392 (51), 315 (12) [M$^+$ − Br], 314 (14), 313 (12) [M$^+$ − Br], 312 (12), 235 (11), 234 (60) [M$^+$ − 2 Br], 232 (10), 189 (34), 117 (28), 116 (17), 95 (12); C$_{16}$H$_{10}$Br$_2$S (394.1): calc. C 48.76, H 2.56, S 8.14; found C 48.71, H 2.57, S 8.17%.

3′-Phenyl-2,2′:5′,2″-terthiophene (13)

A solution of 2-bromothiophene (3.34 g, 20.5 mmol) in diethyl ether (abs., 20 mL) was added dropwise to magnesium chips (598 mg, 24.6 mmol) in boiling diethyl ether (abs., 10 mL). The resulting mixture was heated at reflux for 3 h, allowed to cool to room temperature, and transferred by means of a syringe to the dropping funnel of a second apparatus. The Grignard solution was added dropwise to a suspension of 2,5-dibromo-3-phenyl-thiophene (11) (2.49 g, 7.83 mmol) and 1,3-bis(diphenylphos-phino)propanenickel(II) chloride (42 mg, 7.8×10^{-5} mol) in diethyl ether (abs., 25 mL). The resulting mixture was heated at reflux for 75 h, cooled to room temperature, acidified (2 M HCl, 50 mL), and was extracted with dichloromethane. The combined organic layers were washed with water, saturated NaHCO$_3$ solution, again with water and were dried with MgSO$_4$. After evaporation of the solvent, homocoupling product 2,2′-bithiophene was removed by distillation. The residue was purified by chromatography (SiO$_2$, petroleum ether–dichloromethane 5 : 1) to yield terthiophene 13 (1.35 g, 53%) as an amorphous, yellow solid, mp 85–86 °C; FT-IR (KBr): v = 3096 w, 3077 w, 1488 m, 1413 w, 1230 w, 1042 w, 844 m, 823 m, 762 m, 696 s, 550 w, 472 w cm^{-1}; ^{1}H NMR (500 MHz, CDCl$_3$): δ = 7.34–7.42 (m, 5 H, 2–6$_{Ph}$-H), 7.24 (dd, J = 5.1, 1.2 Hz, 1 H, 5″$_{TTh}$-H), 7.22 (dd, J = 3.7, 1.2 Hz, 1 H, 3″$_{TTh}$-H), 7.18 (dd, J = 5.1, 1.2 Hz, 1 H, 5$_{TTh}$-H), 7.16 (s, 1 H, 4′$_{TTh}$-H), 7.04 (dd, J = 5.1, 3.7 Hz, 1 H, 4″$_{TTh}$-H), 6.99 (dd, J = 3.7, 1.2 Hz, 1 H, 3$_{TTh}$-H), 6.93 (dd, J = 5.1, 3.7 Hz, 1 H, 4$_{TTh}$-H); ^{13}C NMR (126 MHz, CDCl$_3$): δ = 139.6 (C-1$_{Ph}$), 136.86, 136.07, 135.68, 135.44 (C-2,2′,5′,2″$_{TTh}$), 130.5 (C-3′$_{TTh}$), 129.29, 128.45 (C-2,3,5,6$_{Ph}$), 127.90, 127.61, 127.16, 127.00, 126.46, 125.76, 124.67, 123.89 (C-4$_{Ph}$,3–5,4′,3″–5″$_{TTh}$); EI-MS, m/z (%): 326 (14), 325 (22), 324 (100) [M$^+$], 323 (9), 290 (10), 279 (4), 258 (4), 145 (4); C$_{18}$H$_{12}$S$_3$ (324.5): calc. C 66.63, H 3.73, S 29.65; found C 66.38, H 3.76, S 29.37%.

3′,4′-Diphenyl-2,2′:5′,2″-terthiophene (14)

Terthiophene 14 was prepared as described for 13 from 2-thienylmagnesium bromide (14.3 g, 76.2 mmol) in diethyl ether (abs., 50 mL) and a mixture of 2,5-dibromo-3,4-diphenyl-

thiophene (**12**) (5.00 g, 12.7 mmol) and 1,3-bis(diphenyl-phosphino)propanenickel(II) chloride (103 mg, 1.90×10^{-4} mol) in diethyl ether–toluene (3 : 1, abs., 60 mL/100 h). Homo-coupling product 2,2′-bithiophene was removed by distillation. Final purification by chromatography (SiO₂, petroleum ether–dichloromethane 5 : 1) yielded terthiophene **14** (2.40 g, 47%) as yellow microcrystals, mp 188 °C; FT-IR (KBr): $\nu = 3053$ w, 1481 m, 1441 w, 1225 m, 1070 w, 846 m, 827 w, 774 m, 757 m, 692 s, 586 w cm⁻¹; ¹H NMR (500 MHz, CDCl₃): $\delta = 7.19$–7.22 (m, 6 H, 2,4,6$_{Ph}$-H), 7.12 (dd, $J = 5.1$, 1.2 Hz, 2 H, 5,5″$_{TTh}$-H), 7.10–7.12 (m, 4 H, 3,5$_{Ph}$-H), 6.98 (dd, $J = 3.7$, 1.2 Hz, 2 H, 3,3″$_{TTh}$-H), 6.90 (dd, $J = 5.1$, 3.7 Hz, 2 H, 4,4″$_{TTh}$-H); ¹³C NMR (126 MHz, CDCl₃): $\delta = 140.0$ (C-1$_{Ph}$), 136.10, 135.90 (C-2,2′,5′, 2″$_{TTh}$), 131.13 (C-3′,4′$_{TTh}$), 130.72, 128.06 (C-2,3,5,6$_{Ph}$), 127.36, 126.88, 125.88, 125.57 (C-4$_{Ph}$,3–5,5″–5″$_{TTh}$); EI-MS, m/z (%): 402 (17), 401 (28), 400 (100) [M⁺], 399 (4) [M⁺ − H], 366 (3), 365 (3); C₂₄H₁₆S₃ (400.6): calc. C 71.96, H 4.03, S 24.01; found C 71.89, H 3.98, S 24.17%.

5,5″-Dibromo-3′-phenyl-2,2′:5′,2″-terthiophene (16)

Terthiophene **16** was prepared as described for thiophene **11** from NBS (811 mg, 4.56 mmol) in DMF (abs., 10 mL) and 3′-phenyl-2,2′:5′,2″-terthiophene (**13**) (705 mg, 2.17 mmol) in DMF (abs., 10 mL/10 h). Final purification by chromatography (SiO₂, petroleum ether–dichloromethane 5 : 1) yielded dibromo-terthiophene **16** (980 mg, 94%) as an amorphous, yellow solid, mp 79 °C; FT-IR (KBr): $\nu = 3091$ w, 3052 w, 1489 m, 1431 m, 1413 m, 1191 w, 972 m, 839 w, 797 s, 762 s, 698 s, 466 m cm⁻¹; ¹H NMR (500 MHz, CDCl₃): $\delta = 7.35$–7.40 (m, 5 H, 2–6$_{Ph}$-H), 7.05 (s, 1 H, 4′$_{TTh}$-H), 6.99 (d, $J = 3.9$ Hz, 1 H, 3″$_{TTh}$-H or 4″$_{TTh}$-H), 6.94 (d, $J = 3.9$ Hz, 1 H, 3″$_{TTh}$-H or 4″$_{TTh}$-H), 6.88 (d, $J = 3.9$ Hz, 1 H, 3$_{TTh}$-H or 4$_{TTh}$-H), 6.75 (d, $J = 3.9$ Hz, 1 H, 3$_{TTh}$-H or 4$_{TTh}$-H); ¹³C NMR (126 MHz, CDCl₃): $\delta = 140.0$ (C-1$_{Ph}$), 138.1, 137.0, 135.36, 134.72 (C-2,2′,5′,2″$_{TTh}$), 130.78, 129.99, 128.04, 127.16, 126.67, 124.1 (C-4$_{Ph}$,3,4,4′,3″,4″$_{TTh}$), 129.89 (C-3′$_{TTh}$), 129.20, 128.67 (C-2,3,5,6$_{Ph}$), 112.7 (C-5$_{TTh}$), 111.6 (C-5″$_{TTh}$); EI-MS, m/z (%): 485 (13), 484 (59), 483 (21), 482 (100) [M⁺], 481 (10), 480 (50), 277 (13), 245 (11), 201 (11), 200 (10), 161 (13), 139 (14); C₁₈H₁₀Br₂S₃ (482.3): calc. C 44.83, H 2.09, S 19.95; found C 44.86, H 2.12, S 19.71%.

5,5″-Dibromo-3′,4′-diphenyl-2,2′:5′,2″-terthiophene (17)

Terthiophene **17** was prepared as described for thiophene **11** from NBS (1.33 g, 7.49 mmol) in DMF (abs., 10 mL) and 3′,4′-diphenyl-2,2′:5′,2″-terthiophene (**14**) (1.50 g, 3.74 mmol) in DMF (abs., 40 mL/15 h). Final purification by chromatography (SiO₂, petroleum ether–dichloromethane 5 : 1) yielded dibromo-terthiophene **17** (2.07 g, 99%) as yellow microcrystals, mp 204–206 °C (decomp.); FT-IR (KBr): $\nu = 3056$ w, 1511 m, 1482 m, 1443 m, 1428 m, 1212 w, 1071 w, 972 m, 776 s, 760 w, 698 s cm⁻¹; ¹H NMR (500 MHz, CDCl₃): $\delta = 7.18$–7.24 (m, 6 H, 2,4,6$_{Ph}$-H), 7.05–7.10 (m, 4 H, 3,5$_{Ph}$-H), 6.85 (d, $J = 3.9$ Hz, 2 H, 3,3″$_{TTh}$-H or 4,4″$_{TTh}$-H), 6.76 (d, $J = 3.9$ Hz, 2 H, 3,3″$_{TTh}$-H or 4,4″$_{TTh}$-H); ¹³C NMR (126 MHz, CDCl₃): $\delta = 140.4$ (C-1$_{Ph}$), 137.5, 135.2 (C-2,2′,5′,2″$_{TTh}$), 130.58, 129.70, 127.82, 126.0 (C-4$_{Ph}$,3,4,3′,4′,3″,4″$_{TTh}$), 130.53, 128.31 (C-2,3,5,6$_{Ph}$), 112.7 (C-5,5″$_{TTh}$); EI-MS, m/z (%): 562 (7), 561 (14), 560 (55), 559 (22), 558 (100) [M⁺], 556 (43), 365 (5), 364 (8), 332 (5), 308 (4), 182 (13); C₂₄H₁₄Br₂S₃ (558.4): calc. C 51.63, H 2.53, S 17.23; found C 51.74, H 2.55, S 17.12%.

5,5″-Bis(4,5,6,7-tetrahydrobenzo[b]thiophen-2-yl)-3′-phenyl-2,2′:5′,2″-terthiophene (1)

Compound **1** was prepared as described for terthiophene **13** from 4,5,6,7-tetrahydrobenzo[b]thiophen-2-ylmagnesium bromide (1.67 g, 6.90 mmol) in diethyl ether (abs., 30 mL) and a mixture of 5,5″-dibromo-3′-phenyl-2,2′:5′,2″-terthiophene (**16**) (557 mg, 1.15 mmol) and 1,3-bis(diphenylphosphino)-propanenickel(II) chloride (10 mg, 1.8×10^{-5} mol) in diethyl

ether (abs., 30 mL/150 h). Due to its low solubility in diethyl ether, the major portion of **1** could be separated from the reaction mixture by filtration and was separated from homo-coupling product EC2T **19** by chromatography (SiO₂, petrol-eum ether–dichloromethane 5 : 1). Additional material was isolated by extraction and chromatography (SiO₂, petroleum ether–dichloromethane 5 : 1). Final purification by sublimation yielded **1** (311 mg, 45%) as an amorphous orange solid, mp 186–187 °C; FT-IR (KBr): $\nu = 3060$ w, 2929 s, 2839 m, 1520 m, 1496 m, 1444 m, 1347 w, 1140 w, 830 m, 797 s, 763 s, 700 s, 483 w cm⁻¹; ¹H NMR (500 MHz, CDCl₃): $\delta = 7.33$–7.44 (m, 5 H, 2–6$_{Ph}$-H), 7.10 (s, 1 H, 4′$_{TTh}$-H), 7.07 (d, $J = 3.8$ Hz, 1 H, 3″$_{TTh}$-H), 6.99 (d, $J = 3.8$ Hz, 1 H, 4″$_{TTh}$-H), 6.88 (d, $J = 3.8$ Hz, 1 H, 3$_{TTh}$-H), 6.84 (s, 1 H, 3$_{THBTh′}$-H), 6.83 (d, $J = 3.8$ Hz, 1 H, 4$_{TTh}$-H), 6.72 (s, 1 H, 3$_{THBTh}$-H), 2.76 (t, $J = 6.1$ Hz, 2 H, 7$_{THBTh′}$-H), 2.72 (t, $J = 6.1$ Hz, 2 H, 7$_{THBTh}$-H), 2.60 (t, $J = 6.1$ Hz, 2 H, 4$_{THBTh′}$-H), 2.56 (t, $J = 6.1$ Hz, 2 H, 4$_{THBTh}$-H), 1.75–1.89 (m, 8 H, 5,6$_{THBTh}$,5,6$_{THBTh′}$-H); ¹³C NMR (126 MHz, CDCl₃): $\delta = 139.4$ (C-1$_{Ph}$), 138.21, 137.36, 136.27, 136.16, 135.99, 135.63, 135.47, 135.15, 134.77, 133.78, 133.05, 133.03 (C-2,3a,7a$_{THBTh}$,2,3a,7a$_{THBTh′}$,2,5,2′,5′,2″,5″$_{TTh}$), 130.3 (C-3′$_{TTh}$), 129.27, 128.54 (C-2,3,5,6$_{Ph}$), 127.73, 126.94, 126.85, 124.54, 124.48, 124.43, 123.55, 122.99 (C-4$_{Ph}$,3$_{THBTh′}$-3$_{THBTh′}$,3,4,4′,3″,4″$_{TTh}$), 25.53, 25.49 (C-4$_{THBTh}$,4$_{THBTh′}$), 25.07, 25.03 (C-7$_{THBTh}$,7$_{THBTh′}$), 23.52, 23.51 (C-6$_{THBTh}$,6$_{THBTh′}$), 22.79, 22.78 (C-5$_{THBTh}$,5$_{THBTh′}$); EI-MS, m/z (%): 599 (9), 598 (27), 597 (39), 596 (100) [M⁺], 568 (6) [M⁺ − C₂H₄], 540 (3) [M⁺ − 2 C₂H₄], 298 (8) [M²⁺], 284 (4) [M²⁺ − C₂H₄], 270 (8) [M²⁺ − 2 C₂H₄]; C₃₄H₂₈S₅ (596.9): calc. C 68.41, H 4.73, S 26.86; found C 68.12, H 4.75, S 26.66%.

5,5″-Bis(4,5,6,7-tetrahydrobenzo[b]thiophen-2-yl)-3′,4′-diphenyl-2,2′:5′,2″-terthiophene (2)

Compound **2** was prepared as described for **13** from 4,5,6,7-tetrahydrobenzo[b]thiophen-2-ylmagnesium bromide (1.68 g, 7.76 mmol) in diethyl ether (abs., 20 mL) and a mixture of 5,5″-dibromo-3′,4′-diphenyl-2,2′:5′,2″-terthiophene (**17**) (722 mg, 1.29 mmol) and 1,3-bis(diphenylphosphino)propanenickel(II) chloride (11 mg, 2.0×10^{-5} mol) in diethyl ether–toluene (3 : 1, abs., 50 mL/100 h). Due to its low solubility in diethyl ether–toluene, the major portion of **2** could be separated from the reaction mixture by filtration and was separated from homo-coupling product EC2T **19** by fractionating sublimation. Additional material was isolated by extraction, chrom-atography (SiO₂, petroleum ether–dichloromethane 3 : 1), and sublimation to yield **2** (418 mg, 48%) as an amorphous orange solid, mp 277–278 °C; FT-IR (KBr): $\nu = 3058$ w, 2930 s, 2839 w, 1519 w, 1442 m, 1347 w, 792 s, 774 w, 700 s, 493 w cm⁻¹; ¹H NMR (500 MHz, CDCl₃): $\delta = 7.16$–7.24 (m, 6 H, 2,4,6$_{Ph}$-H), 7.07–7.13 (m, 4 H, 3,5$_{Ph}$-H), 6.84 (d, $J = 3.8$ Hz, 2 H, 3,3″$_{TTh}$-H), 6.78 (d, $J = 3.8$ Hz, 2 H, 4,4″$_{TTh}$-H), 6.68 (s, 2 H, 3$_{THBTh}$-H), 2.71 (t, $J = 6.1$ Hz, 4 H, 7$_{THBTh}$-H), 2.54 (t, $J = 6.1$ Hz, 4 H, 4$_{THBTh}$-H), 1.79–1.85 (m, 4 H, 6$_{THBTh}$-H), 1.73–1.79 (m, 4 H, 5$_{THBTh}$-H); ¹³C NMR (126 MHz, CDCl₃): $\delta = 140.0$ (C-1$_{Ph}$), 137.9, 136.12, 135.79, 135.40, 134.3, 133.1 (C-2,3a,7a$_{THBTh}$,2,5,2′,5′,2″,5″$_{TTh}$), 130.98 (C-3′,4′$_{TTh}$), 130.65, 128.19 (C-2,3,5,6$_{Ph}$), 127.49, 126.4, 124.4, 122.8 (C-4$_{Ph}$,3$_{THBTh}$,3,4,3″,4″$_{TTh}$), 25.48 (C-4$_{THBTh}$), 25.02 (C-7$_{THBTh}$), 23.50 (C-6$_{THBTh}$), 22.77 (C-5$_{THBTh}$); EI-MS, m/z (%): 675 (10), 674 (28), 673 (42), 672 (100) [M⁺], 644 (5) [M⁺ − C₂H₄], 616 (2) [M⁺ − 2 C₂H₄], 336 (9) [M²⁺], 322 (3) [M²⁺ − C₂H₄], 308 (7) [M²⁺ − 2 C₂H₄]; C₄₀H₃₂S₅ (673.0): calc. C 71.38, H 4.79, S 23.82; found C 71.08, H 4.81, S 23.87%.

1,3-Bis(5-bromo-2-thienyl)benzo[c]thiophene (18)

Under exclusion of light, a solution of NBS (1.14 g, 6.40 mmol) in DMF (abs., 25 mL) was added dropwise to a solution of 1,3-di(2-thienyl)benzo[c]thiophene (**15**) (955 mg, 3.20 mmol) in DMF (abs., 50 mL) at −20 °C. The resulting mixture was kept for 2 h at −20 °C and was allowed to warm to room temper-

ature overnight. The orange suspension was poured into water. The crude product precipitated during this procedure and was isolated by filtration, washed with water, and dried. Recrystallization from *n*-hexane–trichloromethane 6 : 1 yielded **18** (1.01 g, 69%) as greenish, shining dark red needles, mp 135 °C; FT-IR (KBr): ν = 3062 w, 1529 w, 1489 w, 1433 w, 1190 m, 969 w, 788 s, 778 s, 734 s, 699 m, 582 m cm^{-1}; ^{1}H NMR (500 MHz, CDCl$_3$): δ = 7.85 (dd, J = 7.0, 3.1 Hz, 2 H, 4,7$_{BTh}$-H), 7.15 (dd, J = 7.0, 3.1 Hz, 2 H, 5,6$_{BTh}$-H), 7.10 (d, J = 3.9 Hz, 2 H, 3$_{Th}$-H or 4$_{Th}$-H), 7.07 (d, J = 3.9 Hz, 2 H, 3$_{Th}$-H or 4$_{Th}$-H); ^{13}C NMR (126 MHz, CDCl$_3$): δ = 136.8, 135.5, 125.84 (C-1,3,3a,7a$_{BTh}$,2$_{Th}$), 130.7, 125.93, 125.27, 121.2 (C-4–7$_{BTh}$,3,4$_{Th}$), 112.4 (C-5$_{Th}$); FD-MS, *m/z* (%): 459 (11), 458 (59), 457 (20), 456 (100) [M$^+$], 455 (10), 454 (48); C$_{16}$H$_8$Br$_2$S$_3$ (456.3): calc. C 42.12, H 1.77, S 21.08; found C 42.09, H 1.78, S 20.97%.

1,3-Bis[5-(4,5,6,7-tetrahydrobenzo[*b*]thiophen-2-yl)-2-thienyl]-benzo[c]thiophene (3)

Compound **3** was prepared as described for **13** from 4,5,6,7-tetrahydrobenzo[*b*]thiophen-2-ylmagnesium bromide (1.19 g, 5.48 mmol) in diethyl ether (abs., 20 mL) and a mixture of 1,3-bis(5-bromo-2-thienyl)benzo[*c*]thiophene (**18**) (500 mg, 1.10 mmol) and 1,3-bis(diphenylphosphino)propanenickel(II) chloride (10 mg, 1.8 × 10^{-5} mol) in diethyl ether–toluene (3 : 1, abs., 50 mL/150 h). Due to its low solubility in diethyl ether–toluene, the major portion of oligomer **3** could be separated from the reaction mixture by filtration and was separated from homo-coupling product EC2T **19** by chromatography (aluminium oxide/toluene). Additional material was isolated by extraction and chromatography (aluminium oxide/toluene) to yield **3** (268 mg, 43%) as an amorphous black solid with a tinge of green, mp 228–230 °C; FT-IR (KBr): ν = 3061 w, 2927 s, 2854 m, 1530 w, 1493 w, 1435 w, 1347 w, 1140 w, 829 w, 790 m, 733 m, 586 w cm^{-1}; ^{1}H NMR (500 MHz, CDCl$_3$): δ = 7.97 (dd, J = 6.9, 3.1 Hz, 2 H, 4,7$_{BTh}$-H), 7.23 (d, J = 3.7 Hz, 2 H, 3$_{Th}$-H), 7.15 (dd, J = 6.9, 3.1 Hz, 2 H, 5,6$_{BTh}$-H), 7.10 (d, J = 4.0 Hz, 2 H, 4$_{Th}$-H), 6.90 (s, 2 H, 3$_{THBTh}$-H), 2.77 (t, J = 6.2 Hz, 4 H, 7$_{THBTh}$-H), 2.62 (t, J = 6.2 Hz, 4 H, 4$_{THBTh}$-H), 1.84–1.90 (m, 4 H, 6$_{THBTh}$-H), 1.78–1.84 (m, 4 H, 5$_{THBTh}$-H); ^{13}C NMR (126 MHz, CDCl$_3$): δ = 138.1, 136.33, 135.66, 135.20, 133.1, 129.04, 128.23 (C-1,3,3a,7a$_{BTh}$,2,5$_{Th}$,2,3a,7a$_{THBTh}$), 126.0, 124.88, 124.51, 123.54, 121.7 (C-4–7$_{BTh}$,3,4$_{Th}$,3$_{THBTh}$), 25.56 (C-4$_{THBTh}$), 25.10 (C-7$_{THBTh}$), 23.55 (C-6$_{THBTh}$), 22.82 (C-5$_{THBTh}$); EI-MS, *m/z* (%): 573 (9), 572 (28), 571 (38), 570 (100) [M$^+$], 542 (5) [M$^+$ − C$_2$H$_4$], 285 (12) [M^{2+}], 271 (6) [M^{2+} − C$_2$H$_4$], 257 (7) [M^{2+} − 2 C$_2$H$_4$] (Found: M$^+$, 570.0636, [12]C$_{32}$[1]H$_{26}$[32]S$_5$ requires *M*, 570.0638).

4-(Biphenyl-2-yl)-4-hydroxy-4*H*-cyclopenta[2,1-*b*:3,4-*b′*]-dithiophene (21)

n-BuLi (29.6 mL of a 1.6 M solution in *n*-hexane, 47.3 mmol) was added dropwise to a solution of 2-bromobiphenyl (10.0 g, 43.0 mmol) in *n*-hexane (250 mL) at reflux. The resulting mixture was stirred for 1 h and cooled to −70 °C. During this procedure the lithium salt precipitated and the suspension in *n*-hexane was diluted stepwise by addition of THF (abs., 100 mL). A solution of dithiophenone **20** (8.26 g, 43.0 mmol) in THF (abs., 80 mL) was added dropwise. The reaction mixture was stirred for 1 h at −70 °C and was then allowed to warm to room temperature. After hydrolysis, the layers were separated, the organic layers were washed with water and dried (MgSO$_4$). After evaporation of the solvent, the crude product was purified by chromatography (SiO$_2$, petroleum ether–diethyl ether 5 : 1) to yield **21** (12.4 g, 83%) as colourless microcrystals, mp 169 °C; FT-IR (KBr): ν = 3527 s, 3072 w, 3041 w, 1438 m, 1176 m, 1118 m, 1054 m, 955 s, 864 m, 753 s, 704 s, 663 s, 564 m, 453 w cm^{-1}; ^{1}H NMR (500 MHz, [D$_6$]DMSO): δ = 8.29 (dd, J = 7.9, 1.2 Hz, 1 H, 6$_{BPh}$-H), 7.46 (td, J = 7.7, 1.2 Hz, 1 H, 5$_{BPh}$-H), 7.25 (td, J = 7.5, 1.2 Hz, 1 H, 4$_{BPh}$-H), 7.20 (d, J = 4.7 Hz, 2 H, 2,6$_{CPDTh}$-H), 6.94 (tt, J = 7.5, 1.2 Hz, 1 H, 4′$_{BPh}$-H), 6.83

(t, J = 7.5 Hz, 2 H, 3′,5′$_{BPh}$-H), 6.76 (dd, J = 7.5, 1.2 Hz, 1 H, 3$_{BPh}$-H), 6.71 (d, J = 4.7 Hz, 2 H, 3,5$_{CPDTh}$-H), 6.17 (s, 1 H, O*H*), 6.14 (dd, J = 7.5, 1.2 Hz, 2 H, 2′,6′$_{BPh}$-H); ^{13}C NMR (126 MHz, [D$_6$]DMSO): δ = 158.5, 140.56, 140.35, 139.3, 137.2 (C-1,2,1′$_{BPh}$,3a,4a,7a,7b$_{CPDTh}$), 131.0, 127.82, 127.39, 126.69, 126.26, 126.11, 125.40, 122.3 (C-3–6,2′–6′$_{BPh}$,2,3,5,6$_{CPDTh}$), 77.0 (C-4$_{CPDTh}$); EI-MS, *m/z* (%): 348 (11), 347 (24), 346 (100) [M$^+$], 329 (10) [M$^+$ − OH], 327 (12), 313 (12), 295 (11), 269 (16), 218 (10), 193 [M$^+$ − C$_{12}$H$_9$]; C$_{21}$H$_{14}$S$_2$O (346.5): calc. C 72.80, H 4.07, S 18.51; found C 72.85, H 4.10, S 18.55%.

Spiro[cyclopenta[2,1-*b*:3,4-*b′*]dithiophene-4,9′-fluorene] (22)

Dehydration with boron trifluoride–diethyl ether. A solution of boron trifluoride–diethyl ether (108 µl, 9.02 × 10^{-4} M) in dichloromethane (10 mL) was added dropwise to a solution of alcohol **21** (250 mg, 7.22 × 10^{-4} M) in dichloromethane (150 mL). The resulting mixture was stirred for ten minutes and ethanol (50 mL) and water (150 mL) were successively added. The phases were separated and the aqueous phase was extracted with dichloromethane. The combined dichloromethane layers were washed and dried (MgSO$_4$). After removal of the solvent, the remaining crude product was purified by chromatography (SiO$_2$, petroleum ether–dichloromethane 3 : 1) to yield two fractions. In fraction 1 **22** (142 mg, 60%) was isolated as an amorphous colourless powder, mp 190 °C; FT-IR (KBr): ν = 3095 w, 1447 m, 1087 w, 1002 w, 861 m, 778 w, 739 s, 708 m, 698 m, 668 s, 571 w, 463 w cm^{-1}; ^{1}H NMR (500 MHz, [D$_6$]DMSO): δ = 7.96 (ddd, J = 7.5, 1.2, 0.6 Hz, 2 H, 4,5$_{Fl}$-H), 7.40 (td, J = 7.5, 1.2 Hz, 2 H, 3,6$_{Fl}$-H), 7.34 (d, J = 4.8 Hz, 2 H, 2,6$_{CPDTh}$-H), 7.15 (td, J = 7.5, 1.2 Hz, 2 H, 2,7$_{Fl}$-H), 6.72 (ddd, J = 7.5, 1.2, 0.6 Hz, 2 H, 1,8$_{Fl}$-H), 6.40 (d, J = 4.8 Hz, 2 H, 3,5$_{CPDTh}$-H); ^{13}C NMR (126 MHz, [D$_6$]DMSO): δ = 154.4, 144.7, 141.3, 137.9 (C-3a,4a,7a,7b$_{CPDTh}$,4a,4b,8a,9a$_{Fl}$), 128.20, 127.98, 127.20, 123.2, 121.31, 120.78 (C-2,3,5,6$_{CPDTh}$,1–8$_{Fl}$), 61.5 (C-4$_{CPDTh}$ = 9$_{Fl}$); EI-MS, *m/z* (%): 330 (9), 329 (26), 328 (83) [M$^+$], 327 (100) [M$^+$ − H], 295 (10), 282 (6), 164 (12) [M^{2+}], 163 (6), 148 (13), 141 (7); C$_{21}$H$_{12}$S$_2$ (328.5): calc. C 76.79, H 3.68, S 19.53; found C 76.84, H 3.71, S 19.36%.

In fraction 2 spiro{2-[4-(biphenyl-2-yl)-4*H*-cyclopenta-[2,1-*b*:3,4-*b′*]dithien-4-yl]–cyclopenta[2,1-*b*:3,4-*b′*]dithiophene-4,9′-fluorene} (**23**) (12 mg, 5%) was isolated as the main by-product as a pale yellow powder, mp 163–165 °C; FT-IR (KBr): ν = 3057 w, 1474 w, 1448 m, 1324 w, 1086 w, 1010 w, 856 w, 779 w, 740 s, 697 s, 663 s cm^{-1}; ^{1}H NMR (500 MHz, CDCl$_3$): δ = 7.80 (dd, J = 7.5, 1.2 Hz, 2 H, 4,5$_{Fl}$-H), 7.36 (td, J = 7.5, 1.2 Hz, 2 H, 3,6$_{Fl}$-H), 7.35 (dd, J = 7.5, 1.4 Hz, 1 H, 6$_{BPh}$-H), 7.26 (td, J = 7.5, 1.4 Hz, 1 H, 5$_{BPh}$-H), 7.20 (td, J = 7.5, 1.4 Hz, 1 H, 4$_{BPh}$-H), 7.15 (td, J = 7.5, 1.2 Hz, 2 H, 2,7$_{Fl}$-H), 7.01 (d, J = 5.0 Hz, 1 H, 6$_{CPDTh}$-H), 6.99 (d, J = 5.0 Hz, 2 H, 2,6$_{CPDTh′}$-H), 6.94 (tt, J = 7.5, 1.4 Hz, 1 H, 4′$_{BPh}$-H), 6.90 (dd, J = 7.5, 1.2 Hz, 2 H, 1,8$_{Fl}$-H), 6.87 (d, J = 5.0 Hz, 2 H, 3,5$_{CPDTh′}$-H), 6.86 (td, J = 7.5, 1.4 Hz, 2 H, 3′,5′$_{BPh}$-H), 6.85 (dd, J = 7.5, 1.4 Hz, 1 H, 3$_{BPh}$-H), 6.37 (s, 1 H, 3$_{CPDTh}$-H), 6.34 (d, J = 5.0 Hz, 1 H, 5$_{CPDTh}$-H), 6.23 (dd, J = 7.5, 1.4 Hz, 2 H, 2′,6′$_{BPh}$-H); ^{13}C NMR (126 MHz, [D$_6$]DMSO): δ = 157.7, 145.1, 141.60, 137.56 (C-3a,4a,-7a,7b$_{CPDTh′}$,4a,4b,8a,9a$_{Fl}$), 154.5, 152.9, 147.1, 142.14, 140.56, 139.64, 138.35, 137.48 (C-1,2,1′$_{BPh}$,2,3a,4a,7a,7b$_{CPDTh}$), 131.9, 129.6, 127.20, 126.54, 125.51, 125.37, 122.28, 121.26 (C-3–6,4′$_{BPh}$,3,5,6$_{CPDTh}$), 128.20, 127.80, 127.70, 126.30, 125.17, 123.70, 123.12, 120.0 (C-2′,3′,5′,6′$_{BPh}$,2,3,5,6$_{CPDTh′}$,1–8$_{Fl}$), 62.4, 58.3 (C-4$_{CPDTh}$ = 9$_{Fl}$,4$_{CPDTh′}$); EI-MS, *m/z* (%): 659 (10), 658 (29), 657 (50), 656 (100) [M$^+$], 591 (16), 505 (21), 504 (34), 503 (90) [M$^+$ − C$_{12}$H$_9$], 502 (10), 470 (15), 353 (21), 311 (10), 295 (12); C$_{42}$H$_{24}$S$_4$ (656.9): calc. C 76.79, H 3.68, S 19.53; found C 76.68, H 3.73, S 19.25%.

Dehydration with concentrated hydrochloric acid. A mixture of concentrated hydrochloric acid (1 mL) and acetic acid

(50 mL) was added dropwise to a solution of alcohol **21** (500 mg, 1.44 mmol) in acetic acid (250 mL). The resulting mixture was heated at reflux for 4 h, allowed to cool to room temperature, and poured onto ice water. During this procedure the crude product precipitated and was isolated by filtration, washed with water, and dried. Chromatographic work-up (SiO$_2$, petroleum ether–dichloromethane 3 : 1) yielded **22** (220 mg, 47%) as an amorphous, colourless powder. All analytical data are identical to those obtained for spiro compound **22** generated by dehydration of alcohol **21** in the presence of boron trifluoride–diethyl ether; C$_{21}$H$_{12}$S$_2$ (328.5): calc. C 76.79, H 3.68, S 19.53; found C 76.68, H 3.70, S 19.36%.

2,6-Dibromospiro[cyclopenta[2,1-*b*:3,4-*b*′]dithiophene-4,9′-fluorene] (24)

Fluorene **24** was prepared as described for thiophene **11** from NBS (1.23 g, 6.93 mmol) in DMF (abs., 50 mL) and spiro[cyclopenta[2,1-*b*:3,4-*b*′]dithiophene-4,9′-fluorene] **(22)** (1.11 g, 3.38 mmol) in DMF (abs., 150 mL/5 h). Final purification by chromatography (SiO$_2$, petroleum ether–dichloromethane 5 : 1) yielded **24** (1.52 g, 92%) as colourless microcrystals, mp 280 °C (decomp.); FT-IR (KBr): v = 3081 w, 1450 s, 1366 w, 1355 w, 1174 s, 949 s, 824 s, 741 s, 678 w, 645 m, 460 m, 418 m cm^{-1}; ^{1}H NMR (500 MHz, CDCl$_3$): δ = 7.79 (ddd, J = 7.5, 1.2, 0.6 Hz, 2 H, 4,5$_{Fl}$-H), 7.39 (td, J = 7.5, 1.2 Hz, 2 H, 3,6$_{Fl}$-H), 7.16 (td, J = 7.5, 1.2 Hz, 2 H, 2,7$_{Fl}$-H), 6.86 (ddd, J = 7.5, 1.2, 0.6 Hz, 2 H, 1,8$_{Fl}$-H), 6.44 (s, 2 H, 3,5$_{CPDTh}$-H); ^{13}C NMR (126 MHz, CDCl$_3$): δ = 152.6, 143.6, 141.6, 138.2 (C-3a,4a,7a,7b$_{CPDTh}$,4a,4b,8a,9a$_{Fl}$), 128.35, 127.89, 124.48, 123.54, 120.3 (C-3,5$_{CPDTh}$,1–8$_{Fl}$), 112.1 (C-2,6$_{CPDTh}$), 62.8 (C-4$_{CPDTh}$ = 9$_{Fl}$); EI-MS, m/z (%): 489 (16), 488 (59), 487 (60), 486 (100) [M$^+$], 485 (80) [M$^+$ − H], 484 (52), 483 (35), 407 (24) [M$^+$ − Br], 405 (25) [M$^+$ − Br], 325 (17) [M$^+$ − 2 Br − H], 282 (20), 280 (10), 237 (13), 204 (27), 203 (25), 163 (33), 141 (32), 140 (25), 119 (12); C$_{21}$H$_{10}$Br$_2$S$_2$ (486.2): calc. C 51.87, H 2.07, S 13.19; found C 51.76, H 2.17, S 13.17%.

2,6-Bis(4,5,6,7-tetrahydrobenzo[*b*]thiophenen-2-yl)spiro[cyclopenta[2,1-*b*:3,4-*b*′]dithiophene-4,9′-fluorene] (4)

Oligothiophene **4** was prepared as described for terthiophene **13** from 4,5,6,7-tetrahydrobenzo[*b*]thiophen-2-ylmagnesium bromide (1.34 g, 6.17 mmol) in diethyl ether (abs., 20 mL) and a mixture of 2,6-dibromospiro[cyclopenta[2,1-*b*:3,4-*b*′]-dithiophene-4,9′-fluorene] **(24)** (750 mg, 1.54 mmol) and 1,3-bis(diphenylphosphino)propanenickel(II) chloride (13 mg, 2.4×10^{-5} mol) in diethyl ether–toluene (3 : 1, abs., 50 mL/100 h). Due to its low solubility in diethyl ether–toluene, the major portion of oligomer **4** was isolated from the reaction mixture by filtration and was separated from homocoupling product EC2T **19** by chromatography (SiO$_2$, petroleum ether–dichloromethane 3 : 1). Additional material was isolated by extraction and chromatography (SiO$_2$, petroleum ether–dichloromethane 3 : 1). Final sublimation yielded **4** (222 mg, 24%) as an amorphous yellow solid, mp 288 °C; FT-IR (KBr): v = 3063 w, 2930 m, 2839 w, 1447 m, 1346 w, 826 w, 738 s cm^{-1}; ^{1}H NMR (500 MHz, CDCl$_3$): δ = 7.81 (dd, J = 7.5, 1.2 Hz, 2 H, 4,5$_{Fl}$-H), 7.38 (td, J = 7.5, 1.2 Hz, 2 H, 3,6$_{Fl}$-H), 7.16 (td, J = 7.5, 1.2 Hz, 2 H, 2,3$_{Fl}$-H), 6.95 (dd, J = 7.5, 1.2 Hz, 2 H, 1,8$_{Fl}$-H), 6.72 (s, 2 H, 3$_{THBTh}$-H), 6.39 (s, 2 H, 3,5$_{CPDTh}$-H), 2.66 (t, J = 6.2 Hz, 4 H, 7$_{THBTh}$-H), 2.53 (t, J = 6.2 Hz, 4 H, 4$_{THBTh}$-H), 1.77–1.83 (m, 4 H, 6$_{THBTh}$-H), 1.71–1.77 (m, 4 H, 5$_{THBTh}$-H); ^{13}C NMR (126 MHz, CDCl$_3$): δ = 154.6, 144.9, 141.6, 139.0 (C-3a,4a,7a,7b$_{CPDTh}$,4a,4b,8a,9a$_{Fl}$), 136.54, 136.01, 134.86, 133.93 (C-2,6$_{CPDTh}$,2,3a,7a$_{THBTh}$), 127.97, 127.78, 123.84, 123.56, 120.1, 117.3 (C-3,5$_{CPDTh}$,3$_{THBTh}$,1-8$_{Fl}$), 62.5 (C-4$_{CPDTh}$ = 9$_{Fl}$), 25.46 (C-4$_{THBTh}$), 24.98 (C-7$_{THBTh}$), 23.48 (C-6$_{THBTh}$), 22.75 (C-5$_{THBTh}$); EI-MS, m/z (%): 603 (6), 602 (20), 601 (35), 600 (100) [M$^+$], 571 (4), 300 (12) [M^{2+}]; C$_{37}$H$_{28}$S$_4$ (600.9): calc. C 73.96, H 4.70, S 21.35; found C 73.79, H 4.69, S 21.13%.

2,6-Bis[5-(4,5,6,7-tetrahydrobenzo[*b*]thiophen-2-yl)-2-thienyl]-spiro[cyclopenta[2,1-*b*:3,4-*b*′]dithiophene-4,9′-fluorene] (5)

A solution of 5-(4,5,6,7-tetrahydrobenzo[*b*]thiophen-2-yl)-2-trimethylstannylthiophene (854 mg, 2.26 mmol) in DMF (abs., 10 mL) was added dropwise to a suspension of fluorene **24** (500 mg, 1.03 mmol), bis(triphenylphosphine)palladium(II) dichloride (72 mg, 1.03×10^{-4} mol) and copper(II) oxide (168 mg, 2.06 mmol) in DMF (abs., 25 mL) at 100 °C. The resulting mixture was stirred for 20 h, allowed to cool to room temperature, hydrolyzed, and extracted with dichloromethane. The combined organic layers were washed with saturated NaHCO$_3$ solution and dried with MgSO$_4$. After evaporation of the solvent the remaining mixture of **5** and homocoupling product EC4T **6** was separated by chromatography (SiO$_2$, petroleum ether–dichloromethane 3 : 1). Further sublimation finally yielded **5** (550 mg, 70%) as an amorphous bright red solid, mp 330–331 °C (decomp.); FT-IR (KBr): v = 3062 w, 2929 m, 2837 w, 1447 m, 1347 w, 827 w, 788 s, 735 s cm^{-1}; ^{1}H NMR (500 MHz, CDCl$_3$): δ = 7.84 (dd, J = 7.5, 1.2 Hz, 2 H, 4,5$_{Fl}$-H), 7.40 (td, J = 7.5, 1.2 Hz, 2 H, 3,6$_{Fl}$-H), 7.18 (td, J = 7.5, 1.2 Hz, 2 H, 2,7$_{Fl}$-H), 6.96 (dd, J = 7.5, 1.2 Hz, 2 H, 1,8$_{Fl}$-H), 6.95 (d, J = 3.7 Hz, 2 H, 3$_{Th}$-H or 4$_{Th}$-H), 6.90 (d, J = 3.7 Hz, 2 H, 3$_{Th}$-H or 4$_{Th}$-H), 6.74 (s, 2 H, 3$_{THBTh}$-H), 6.48 (s, 2 H, 3,5$_{CPDTh}$-H), 2.72 (t, J = 5.7 Hz, 4 H, 7$_{THBTh}$-H), 2.56 (t, J = 5.7 Hz, 4 H, 4$_{THBTh}$-H), 1.80–1.86 (m, 4 H, 6$_{THBTh}$-H), 1.74–1.80 (m, 4 H, 5$_{THBTh}$-H); ^{13}C NMR (126 MHz, CDCl$_3$): δ = 155.1, 144.6, 141.6, 138.5 (C-3a,-4a,7a,7b$_{CPDTh}$,4a,4b,8a,9a$_{Fl}$), 137.01, 136.56, 136.21, 135.82, 135.42, 133.1 (C-2,6$_{CPDTh}$,2,5$_{Th}$,2,3a,7a$_{THBTh}$), 128.14, 127.89, 124.24, 123.79, 123.42, 120.2, 117.7 (C-3,5$_{CPDTh}$,3,4$_{Th}$,3$_{THBTh}$,1–8$_{Fl}$), 62.4 (C-4$_{CPDTh}$ = 9$_{Fl}$), 25.49 (C-4$_{THBTh}$), 25.03 (C-7$_{THBTh}$), 23.49 (C-6$_{THBTh}$), 22.76 (C-5$_{THBTh}$); EI-MS, m/z (%): 768 (5), 767 (12), 766 (27), 765 (38), 764 (100) [M$^+$], 382 (10) [M^{2+}], 368 (4) [M^{2+} − C$_2$H$_4$], 354 (4) [M^{2+} − 2 C$_2$H$_4$]; C$_{45}$H$_{32}$S$_6$ (765.2): calc. C 70.64, H 4.22, S 25.14; found C 70.63, H 4.22, S 24.96%.

Acknowledgements

References

1 (*a*) D. Fichou, *Handbook of Oligo- and Polythiophenes*, Wiley-VCH, Weinheim, 1999; (*b*) P. Bäuerle, Oligothiophenes, in *Electronic Materials: The Oligomer Approach* (Eds.: K. Müllen and G. Wegner), Wiley-VCH, Weinheim, 1998, p. 105; (*c*) J. M. Tour, *Chem. Rev.*, 1996, **96**, 537; (*d*) J. Roncali, *Chem. Rev.*, 1997, **97**, 173.

2 (*a*) G. Horowitz, *Adv. Mater.*, 1998, **10**, 365; (*b*) W. Li, H. E. Katz, A. J. Lovinger and J. G. Laquindanum, *Chem. Mater.*, 1999, **11**, 458; (*c*) F. Garnier, R. Hajlaoui, A. El Kassmi, G. Horowitz, L. Laigre, W. Porzio, M. Armanini and F. Provasoli, *Chem. Mater.*, 1998, **10**, 3334; (*d*) C. D. Dimitrakopoulos, B. K. Furman, T. Graham, S. Hegde and S. Purushothaman, *Synth. Met.*, 1998, **92**, 47; (*e*) G. Barbarella, P. Ostoja, P. Maccagnani, O. Pudova, L. Antolini, D. Casarini and A. Bongini, *Chem. Mater.*, 1998, **10**, 3683.

3 (*a*) U. Mitschke and P. Bäuerle, *J. Mater. Chem.*, 2000, **10**, 1471; (*b*) M. G. Harrison and R. H. Friend, Optical Applications, in *Electronic Materials: The Oligomer Approach* (Eds.: K. Müllen and G. Wegner), Wiley-VCH, Weinheim, 1998, p. 515; (*c*) Y. Shirota, *J. Mater. Chem.*, 2000, **10**, 1.

4 (*a*) U. Mitschke, E. Mena Osteritz, T. Debaerdemaeker, M. Sokolowski and P. Bäuerle, *Chem. Eur. J.*, 1998, **4**, 2211; (*b*) U. Mitschke, T. Debaerdemaeker and P. Bäuerle, *Eur. J. Org. Chem.*, 2000, 425.

5 (*a*) P. Bäuerle, U. Mitschke, E. Mena-Osteritz, M. Sokolowski, D. Müller, M. Groß and K. Meerholz, *Proc. SPIE Int. Soc. Opt. Eng.*, 1998, **3476**, 32; (*b*) G. Gigli, G. Barbarella, L. Favaretto, F. Cacialli and R. Cingolani, *Appl. Phys. Lett.*, 1999, **75**, 439; (*c*) V. Gebhardt, A. Bacher, M. Thelakkat, U. Stalmach, H. Meier, H.-W. Schmidt and D. Haarer, *Adv. Mater.*, 1999, **11**, 119.

6 (*a*) W. A. Schoonveld, R. W. Stok, J. W. Weijtmans, J. Vrijmoeth, J. Wildeman and T. M. Klapwijk, *Synth. Met.*, 1997, **84**, 583; (*b*) C. Y. Yang, Y. Yang and S. Hotta, *Mol. Cryst. Liq. Cryst.*, 1995, **270**,

113; (*c*) A. Soukopp, K. Glöckler, P. Kraft, S. Schmitt, M. Sokolowski, E. Umbach, E. Mena-Osteritz, P. Bäuerle and E. Hädicke, *Phys. Rev. B*, 1998, **58**, 13882; (*d*) A. Soukopp, K. Glöckler, P. Bäuerle, M. Sokolowski and E. Umbach, *Adv. Mater.*, 1996, **8**, 902.

7 P. Bäuerle, *Adv. Mater.*, 1992, **4**, 102.

8 J. Kankare, J. Lukkari, P. Pasanen, R. Sillanpää, H. Laine and K. Harmaa, *Macromolecules*, 1994, **27**, 4327.

9 Fuji Electric Co., Ltd., JP 63,158,564/1988 (*Chem. Abstr.*, 1989, **110**, 85430c); Fuji Electric Co., Ltd., JP 63,170,652–63,170,653/1988 (*Chem. Abstr.*, 1989, **110**, 85391r–85392s); Fuji Electric Co., Ltd., JP 63,178,246/1988 (*Chem. Abstr.*, 1989, **110**, 85395v); Fuji Electric Co., Ltd., JP 63,183,451/1988 (*Chem. Abstr.*, 1989, **111**, 48041b); Fuji Electric Co., Ltd., JP 63,188,147/1988 (*Chem. Abstr.*, 1989, **110**, 85402v); Fuji Electric Co., Ltd., JP 63,192,049–63,192,050/1988 (*Chem. Abstr.*, 1989, **110**, 85405y, 85407a); Fuji Electric Co., Ltd., JP 63,214,758/1988 (*Chem. Abstr.*, 1989, **110**, 85424d); Fuji Electric Co., Ltd., JP 63,287,957–63,287,960/1988 (*Chem. Abstr.*, 1989, **111**, 15316s–15319v); Fuji Electric Co., Ltd., JP 63,296,054–63,296,055/1988 (*Chem. Abstr.*, 1989, **111**, 15326v–15327w).

10 (*a*) T.-A. Chen, R. A. O'Brien and R. D. Rieke, *Macromolecules*, 1993, **26**, 3462; (*b*) M. R. Andersson, D. Selse, M. Berggren, H. Järvinen, T. Hjertberg, O. Inganäs, O. Wennerström and J.-E. Österholm, *Macromolecules*, 1994, **27**, 6503; (*c*) D. J. Guerrero, X. Ren and J. P. Ferraris, *Chem. Mater.*, 1994, **6**, 1437; (*d*) M. Ueda, Y. Miyaji, T. Ito, Y. Oba and T. Sone, *Macromolecules*, 1991, **24**, 2694; (*e*) M.-A. Sato, S. Tanaka and K. Kaeriyama, *Makromol. Chem.*, 1989, **190**, 1233; (*f*) M. Onada, H. Nakayama, S. Morita and K. Yoshino, *J. Appl. Phys.*, 1993, **73**, 2859; (*g*) F. Martínez, J. Retuert and G. Neculqueo, *Int. J. Polym. Mater.*, 1995, **28**, 51.

11 (*a*) L. Robitaille, M. Leclerc and C. L. Callender, *Chem. Mater.*, 1993, **5**, 1755; (*b*) J. P. Ferraris, M. M. Eissa, I. D. Brotherston, D. C. Loveday and A. A. Moxey, *J. Electroanal. Chem.*, 1998, **459**, 57; (*c*) J. P. Ferraris, M. M. Eissa, I. D. Brotherston and D. C. Loveday, *Chem. Mater.*, 1998, **10**, 3528; (*d*) Y. Gofer, J. G. Kilian, H. Sarker, T. O. Poehler and P. C. Searson, *J. Electroanal. Chem.*, 1998, **443**, 103.

12 (*a*) R. Kiebooms, P. Adriaensens, D. Vanderzande, J. Gelan, M. J. Swann, D. Bloor, C. J. Drury and G. M. Brooke, *Macromolecules*, 1996, **29**, 5981; (*b*) M. Lapkowski, R. Kiebooms, A. Pron, O. Chauvet, J. Gelan, D. Vanderzande and S. Lefrant, *Synth. Met.*, 1997, **84**, 413.

13 (*a*) P. Bäuerle, G. Götz, P. Emele and H. Port, *Adv. Mater.*, 1992, **4**, 564; (*b*) D. Lorcy and M. P. Cava, *Adv. Mater.*, 1992, **4**, 562; (*c*) S. Musmanni and J. P. Ferraris, *J. Chem. Soc., Chem. Commun.*, 1993, 172; (*d*) R. H. L. Kiebooms, P. J. A. Adriaensens, D. J. M. Vanderzande and J. M. J. V. Gelan, *J. Org. Chem.*, 1997, **62**, 1473; (*e*) D. Vangeneugden, R. Kiebooms, P. Adriaensens, D. Vanderzande, J. Gelan, J. Desmet and G. Huyberechts, *Acta Polym.*, 1998, **49**, 687.

14 A. K. Mohanakrishnan, M. V. Lakshmikantham, C. McDougal, M. P. Cava, J. W. Baldwin and R. M. Metzger, *J. Org. Chem.*, 1998, **63**, 3105.

15 R. Wu, J. S. Schumm, D. L. Pearson and J. M. Tour, *J. Org. Chem.*, 1996, **61**, 6906.

16 (*a*) N. Johansson, J. Salbeck, J. Bauer, F. Weissörtel, P. Bröms, A. Andersson and W. R. Salaneck, *Adv. Mater.*, 1998, **10**, 1136; (*b*) J. Salbeck, N. Yu, J. Bauer, F. Weissörtel and H. Bestgen, *Synth. Met.*, 1997, **91**, 209; (*c*) F. Steuber, J. Staudigel, M. Stössel, J. Simmerer, A. Winnacker, H. Spreitzer, F. Weissörtel and J. Salbeck, *Adv. Mater.*, 2000, **12**, 130; (*d*) K.-H. Weinfurtner, F. Weissörtel, G. Harmgarth and J. Salbeck, *Proc. SPIE Int. Soc. Opt. Eng.*, 1998, **3476**, 40.

17 M. Thelakkat and H.-W. Schmidt, *Polym. Adv. Technol.*, 1998, **9**, 429.

18 J.-P. Monthéard and J.-F. Delzant, *Synth. Commun.*, 1984, **14**, 293.

19 K. Tamao, S. Kodama, I. Nakajima, M. Kumada, A. Minato and K. Suzuki, *Tetrahedron*, 1982, **38**, 3347.

20 C. van Pham, A. Burkhardt, R. Shabana, D. D. Cunningham, H. B. Mark, Jr. and H. Zimmer, *Phosphorus, Sulfur Silicon Relat. Elem.*, 1989, **46**, 153.

21 V. Duchenet, C. G. Andrieu, J. M. Catel and G. Le Coustumer, *Phosphorus, Sulfur Silicon Relat. Elem.*, 1996, **118**, 117.

22 J. K. Herrema, J. Wildeman, F. van Bolhuis and G. Hadziioannou, *Synth. Met.*, 1993, **60**, 239.

23 (*a*) S. Gronowitz and B. Eriksson, *Ark. Kemi*, 1963, **21**, 335; (*b*) S. Gronowitz, J. E. Skramstad and B. Eriksson, *Ark. Kemi*, 1967, **28**, 99; (*c*) P. Jordens, G. Rawson and H. Wynberg, *J. Chem. Soc. (C)*, 1970, 273.

24 S. Gronowitz, P. Björk, J. Malm and A.-B. Hörnfeldt, *J. Organomet. Chem.*, 1993, **460**, 127.

25 D. Delabouglise, M. Hmyene, G. Horowitz, A. Yassar and F. Garnier, *Adv. Mater.*, 1992, **4**, 107.

26 R. S. Becker, J. S. de Melo, A. L. Maçanita and F. Elisei, *J. Phys. Chem.*, 1996, **100**, 18683.

27 (*a*) A. Kraft, A. C. Grimsdale and A. B. Holmes, *Angew. Chem., Int. Ed.*, 1998, **37**, 402; (*b*) *Organic Electroluminescent Materials and Devices* (Eds.: S. Miyata and H. S. Nalwa), Gordon and Breach Publishers, Amsterdam, 1997.

28 R. N. Adams, *Electrochemistry at Solid Electrodes*, Marcel Dekker, New York, 1969, p. 146.

29 D. Müller, M. Gross, U. Mitschke, P. Bäuerle and K. Meerholz, *Adv. Mater.*, in preparation.

30 H. G. O. Becker, H. Böttcher, F. Dietz, A. V. El'cov, D. Rehorek, G. Roewer, K. Schiller, O. P. Studzinskij and H.-J. Timpe, *Einführung in die Photochemie*, 2nd edn., Thieme, Stuttgart, New York, 1983.

31 J. N. Demas and G. A. Crosby, *J. Phys. Chem.*, 1971, **75**, 991.

32 G. Brauer, *Handbuch der präp. Anorg. Chemie*, Vol. III, Ferdinand Enke Verlag, Stuttgart, 1981, p. 1729 and p. 2014.

33 S. Gronowitz, *Acta Chem. Scand.*, 1959, **13**, 1045.